Vertical distribution of particle-phase dicarboxylic acids, oxoacids and α-dicarbonyls in the urban boundary layer based on the 325-meter tower in Beijing

Wanyu Zhao[1,5,6], Hong Ren[2], Kimitaka Kawamura[3,5], Huiyun Du[1,6], Xueshun Chen[1,6], Siyao Yue[1,6], Qiaorong Xie[1,6], Lianfang Wei[1,6], Ping Li[1,6], Xin Zeng[4], Shaofei Kong[4], Yele Sun[1], Zifa Wang[1], and Pingqing Fu[2*]

[1]State Key Laboratory of Atmospheric Boundary Layer Physics and Atmospheric Chemistry, Institute of Atmospheric Physics, Chinese Academy of Sciences, Beijing 100029, China

[2]Institute of Surface-Earth System Science, School of Earth System Science, Tianjin University, Tianjin 300072, China

[3]Chubu Institute for Advanced Studies, Chubu University, Kasugai 487-8501, Japan

[4]Department of Atmospheric Science, School of Environmental Sciences, China University of Geosciences, Wuhan, 430074, China

[5]Institute of Low Temperature Science, Hokkaido University, Sapporo 060-0819, Japan

[6]College of Earth and Planetary Sciences, University of Chinese Academy of Sciences, Beijing 100049, China

Correspondence to: Pingqing Fu (fupingqing@tju.edu.cn)

Abstract. Vertical distributions of dicarboxylic acids, oxoacids, α-dicarbonyls and other organic tracer compounds in fine aerosols ($PM_{2.5}$) were investigated at three heights (8 m, 120 m and 260 m) based on a 325-meter meteorological tower in urban Beijing in the summer of 2015. Results showed that the concentrations of oxalic acid (C_2), the predominant diacid, were more abundant at 120 m (210 ± 154 ng m^{-3}) and 260 m (220 ± 140 ng m^{-3}) than those at the ground surface (160 ± 90 ng m^{-3}). Concentrations of phthalic acid (Ph) decreased with the increase of height, indicating that local vehicular exhausts were the main contributor. Positive correlations were noteworthy for C_2/total diacids with mass ratios of C_2 to main oxoacids (Pyr and ωC_2) and α-dicarbonyls (Gly and MeGly) in polluted days ($0.42 \leq r^2 \leq 0.65$), especially at the ground level. In clean days, the ratios of carbon content in oxalic acid to water-soluble organic carbon (C_2-C/WSOC) showed larger values at 120 m and 260 m than those at the ground surface. However, in polluted days, the C_2-C/WSOC ratio mainly reached its maximum at the ground level. These phenomena may indicate the enhanced contribution of aqueous-phase oxidation to oxalic acid in polluted days. Combined with the influence of wind field, total diacids, oxoacids and α-dicarbonyls decreased by 22% − 58% under the

control on anthropogenic activities during the 2015 Victory Parade period. Furthermore, the PMF results showed that the secondary formation routes (secondary sulfate formation and secondary nitrate formation) were the dominant contributors (37 − 44%) to organic acids, followed by biomass burning (25 − 30%) and motor vehicles (18 − 24%). In this study, the organic acids at the ground level were largely associated with local traffic emissions, while the long-range atmospheric transport followed by photochemical aging contributed more to diacids and related compounds in the urban boundary layer than the ground surface in Beijing.

1 Introduction

Organic aerosols typically make up 20 – 50 % of the mass concentrations of atmospheric fine aerosols ($PM_{2.5}$) at continental midlatitudes. A large portion of organic aerosols is water-soluble, contributing 20 – 75% to the carbon mass of aerosols emitted from uncompleted combustion sources (Falkovich et al., 2005; Pathak et al., 2011; Graham et al., 2002). Low molecular weight (LMW) dicarboxylic acids and related compounds are water-soluble and are found abundantly in urban (Wang et al., 2012; Zhao et al., 2018), mountainous (Kawamura et al., 2013; Cong et al., 2015), remote marine (Mochida et al., 2007; Wang et al., 2006c; Fu et al., 2013a; Yang et al., 2020), and the Arctic (Kawamura et al., 2010; Kawamura et al., 1996) aerosols, and also in snow, rain and fog waters (Sempére and Kawamura, 1994; Kawamura et al., 2001; Zhao et al., 2019a; Zhao et al., 2019b).

Owing to high water-solubility and hygroscopicity, dicarboxylic acids play an important role in aerosol chemistry via atmospheric processing (e.g., iron catalyzed photolysis and secondary component formation) (Laskin et al., 2012; Drozd et al., 2014; Pavuluri and Kawamura, 2012) and in Earth's climate by enhancing hygroscopic behavior of aerosols to act as cloud condensation nuclei (Andreae and Rosenfeld, 2008; Bilde et al., 2015; Kanakidou et al., 2005). Dicarboxylic acids and related compounds are largely produced by secondary oxidation pathways, including photochemical (Kawamura and Gagosian, 1987; Pavuluri et al., 2015) and aqueous oxidation (Carlton et al., 2007; Ervens and Volkamer, 2010) in the atmosphere. In addition, they are directly emitted from natural emissions such as marine plankton activities (Rinaldi et al.,

2011; Tedetti et al., 2006) and anthropogenic sources including biomass burning (Legrand and Angelis, 1996; Narukawa et al., 1999), vehicular exhausts and fossil fuel combustion (Rogge et al., 1993; Kawamura and Kaplan, 1987).

Previous field measurements mostly focused on organic aerosols at the ground surface. Vertical measurements have been extensively conducted at a global scale since the early 2010s (Han et al., 2015; Hu et al., 2011; Andreae et al., 2012; Chi et al., 2013). The Amazon Tall Tower Observatory (ATTO) was established ~150 km northeast of the city of Manaus, Brazil for comprehensive studies of meteorology (Morton et al., 2014; Quesada et al., 2012; Sun et al., 2011), trace gases (Andreae et al., 2012; Trebs et al., 2012), aerosol compositions (Andreae et al., 2012; Yáñez-Serrano et al., 2015; Yáñez-Serrano et al., 2018; Rizzo et al., 2013; Saturno et al., 2018), and ecology (Pöhlker et al., 2019; Quesada et al., 2012) to investigate long-term trends of the Amazonian hydrological and biogeochemical cycling linked with the human perturbation (Andreae et al., 2015). The 304 m tower of the Zotino Tall Tower Observatory (ZOTTO) in central Siberia serves as a basis for monitoring biogeochemical gases (Chi et al., 2013; Mikhailov et al., 2017; Winderlich et al., 2010), aerosol characteristics (Chi et al., 2013; Heintzenberg et al., 2011; Mikhailov et al., 2017) and atmospheric transport (Mikhailov et al., 2017) at a wide range of spatial and temporal scales.

Beijing, the capital of China, is surrounded by highly industrialized and urbanized areas (Xia et al., 2007) and has encountered severe haze events, especially in winter (Huang et al., 2014; Wang et al., 2016; Xie et al., 2020). The haze pollution in Beijing is characterized by regional transport (Zhao et al., 2013) followed by the accumulation of local emissions, and is mainly driven by secondary aerosol formation, which accounts for 30 – 77% of total aerosol mass and 44 – 71% of organic aerosol mass in the fine mode (Huang et al., 2014). Field measurements in urban regions at the ground level are heavily influenced by local sources, which bring uncertainties to quantify the relative contribution of regional transport to air quality. However, the vertical analysis can largely make up for the deficiency of surface observation and provide more physical and chemical information about the atmospheric process and structure. Guo et al. (2016) found that the thermal stratification was clearly observed for the urban boundary-layer in severe haze events, and the vertical distributions of air pollutants were largely affected by the structure of the atmospheric boundary layer. Guinot et al. (2006) reported that the

urban canopy layer (60 ~ 90 m) in Beijing is associated with the height of buildings and the mean width of street, both factors directly influencing local turbulence and pollutants dispersion. Furthermore, vertical measurements of extinction coefficient, gas precursors and aerosol compositions (e.g., organic compounds, sulfate and nitrate) (Wang et al., 2018; Zhang et al., 2017) have also been conducted in detail at the 325 m meteorological tower in Beijing to better understand the formation and evolution mechanisms of haze events. High loadings of dicarboxylic acids in the atmosphere are closely linked to substantial anthropogenic activities (Kawamura et al., 2013; Wang et al., 2012; Wang et al., 2006b; Zhao et al., 2018). Understanding of the vertical characteristics of organic components in aerosols is important to elaborate the oxidation mechanism, and their interactions with the lower boundary layer in haze events. The vertical investigation of organic aerosols at a molecular level is far from complete, especially for diacids and related compounds.

This study investigates, for the first time, the vertical distributions of LMW dicarboxylic acids, oxoacids and α-dicarbonyls in $PM_{2.5}$ collected at Beijing during August to September 2015, along with the analyses of ions, water-soluble organic carbon (WSOC), organic carbon (OC), elemental carbon (EC) and tracer compounds like levoglucosan (biomass burning tracer) and isoprene-oxidation products. The sources, aerosol chemistry, atmospheric long-range transport, and the effects of emission control on anthropogenic activities were discussed.

2. Experimental methods

2.1 Aerosol sampling

The three-layer sampling was performed at the rooftop of a two-story building (the ground level, 8 m a.g.l.) and two platforms (120 m and 260 m a.g.l.) on the 325-meter meteorological tower in the campus of the Institute of Atmospheric Physics, Chinese Academy of Sciences (39°58’28’’N, 116°22’16’’E) (Fig. 1), a typical urban location influenced by traffic and cooking emissions in Beijing (Sun et al., 2012; Yue et al., 2017). $PM_{2.5}$ samples were collected onto pre-heated (450°C, 6 hours) quartz-fiber filters (Pallflex) by using three high-volume air samplers (TISCH, USA), which were deployed directly at the ground surface (8 m), 120 m, and 260 m on the tower. All of the samplers were run at an airflow rate of 1.0 m^3/min for 23 hours during the 2015 Victory Parade period (from 15 August to 10 September, n = 77). The sampling time was divided

into the first non-restriction period, the restriction and the second non-restriction periods. Field blanks were collected in each period at three sampling layers by placing filters on the samplers for half a minute without pumping. After the campaign, all filters were stored at −20°C until analysis.

2.2 Analyses of diacids and related compounds

The quantitative determinations of diacids, oxoacids and α-dicarbonyls in $PM_{2.5}$ samples followed the analytical measurements as described elsewhere (Kawamura and Ikushima, 1993; Kawamura and Bikkina, 2016). Briefly, 3.14 cm^2 of each filter sample was extracted with Milli-Q water under ultrasonication for water-soluble organic acids. Next these extracts were concentrated to dryness using a rotary evaporator under vacuum and reacted with 14% BF_3/n-butanol at 100°C for 1 hour. Finally, the derivatives were dissolved in *n*-hexane and were analyzed by using a gas chromatograph (GC, Agilent 6980) equipped with an HP-5 column (0.2 mm × 25 m, 0.5 μm film thickness) and an FID detector. The same analytical method was also used for field blank filters. The concentrations of targeted organic acids in this study were corrected for the field blanks, and their recoveries were > 85%.

2.3 Determinations of organic tracers

Small discs of filters were extracted with dichloromethane/methanol (2:1, v/v). The extracts were filtered through quartz wool, concentrated under vacuum and blew to dryness. Derivatization was the reaction with N,O-bis-(trimethylsilyl) trifluoroacetamide (BSTFA) containing pyridine (5:1) and 1% trimethylsilyl chloride at 70°C for 3 hours. Finally, the derivatives were added with *n*-hexane containing the internal standard of C_{13} *n*-alkane (1.43 ng μL^{-1}) before the gas chromatography/mass spectroscopy (GC/MS). The GC/MS analysis was performed using a Hewlett-Packard model 7890A GC coupled to an Agilent model 5975C mass selective detector (MSD). The recoveries of levoglucosan and isoprene SOA tracers were better than 80%, and both concentrations were corrected for the field blanks. Detailed analytical methods can be found in previous studies (Fan et al., 2020; Fu et al., 2013b).

2.4 Inorganic ions, WSOC, OC and EC measurements

For the analysis of ions, a filter aliquot of each sample was extracted by ultrapure Milli-Q water under ultrasonication. Then the extracts were determined for cations (Na^+, K^+, NH_4^+, Ca^{2+}, Mg^{2+}) and anions (F^-, Cl^-, NO_2^-, SO_4^{2-}, NO_3^-) by an Ion Chromatography (Dionex Aquion, Thermo Scientific, America). Data of cations and anions were determined simultaneously. The extraction step of WSOC is similar to that of ions, but the material of extraction bottle is glass. Next the extracts were measured for WSOC by a Shimadzu TOC-V CPH total carbon analyzer with the limit of detection of 0.1 μgC m^{-3} (Kawamura et al., 2013). OC and EC were determined using thermal optical reflectance (TOR) following the Interagency Monitoring of Protected Visual Environments (IMPROVE) protocol on a DRI Model 2001 Thermal/Optical Carbon Analyzer (Chow et al., 2005). The limit of detection for the carbon analysis is 0.8 and 0.4 μgC cm^{-2} for OC and EC respectively, with a precision better than 10% for total carbon (TC). Mass concentrations of ions, WSOC, OC and EC reported in the present study were all corrected for the field blanks.

2.5 FLEXPART-WRF modeling

The Lagrangian particle dispersion model FLEXPART-WRF can be used to quantify the impact of potential source regions (Brioude et al., 2013). Atmospheric particles were released at the height of 8 m at the sampling site every three hours a day. Backward simulation was run for three days and the residence time of aerosols was calculated.

2.6 Meteorological parameters

The meteorological data, such as temperature (T), relative humidity (RH) and wind (wind speed and direction), were also obtained at same locations, except for the highest sampling site (280 m a.g.l.). The wind speed and direction at the ground level were almost same in the field campaign (Fig. S1a). During the restriction period in Beijing, the organic compounds at 120 m were largely influenced by clean northern wind, while the aerosol particles at 280 m were mainly affected by the northwestern wind and accompanied by the influence of polluted southern and southeastern winds. Different from the second

non-restriction period, the air quality at 120 m and 280 m were largely associated with southwestern wind from industrializations in the first non-restriction episode.

3. Results and Discussion

3.1 OC and EC

EC is a useful tracer for incomplete combustion emissions, including vehicle exhausts, biomass burning and fossil fuel combustion (Turpin and Huntzicker, 1991; Bond et al., 2013), while OC is either emitted from primary sources or produced by secondary oxidation pathways in the atmosphere (Clarke et al., 2004). Previous studies found that relatively large OC/EC ratio is associated with biomass burning (7.3), whereas lower value is linked to vehicular exhausts (1.1) (Sandradewi et al., 2008). And Watson et al. (2001) reported the OC/EC ratio of 4.0 attributed to fossil fuel combustion.

Figure 2 shows the daily variations of OC, EC, OC/EC, SOC and POC, SOC/POC in $PM_{2.5}$ collected at the ground level, 120 m and 260 m in summer. During the field campaign, concentration level of EC was considerably lower than OC, but their variation trends were similar (Fig. 2a & 2b). The average value of OC/EC ratios at ground surface and upper layers nearly constant, which showed relative difference < 0.5 and a slightly higher mean value (7.5 ± 1.5) at 8 m (Table S1). Air quality in the North China Plain is considerably influenced by biomass burning after summer harvest (Fu et al., 2012; Sun et al., 2016; Desyaterik et al., 2013). The variations of OC/EC ratios in this study covered the value known for motor exhausts, fossil fuel combustion and biomass burning sources (Fig. 2c). Good linear relationships were observed for OC with EC ($0.59 \leq r^2 \leq 0.78$) (Fig. 3), which indicated an important anthropogenic combustion source to OC.

Secondary organic carbon (SOC) is derived from various physical and chemical transformation processing, like gas/particle partitioning of semi-volatile compounds (Hallquist et al., 2009). Owing to the complexities of SOC formation routes, there is no valid direct analytical measurement to determine the atmospheric concentration of SOC. Primary organic carbon (POC) is directly emitted from natural and anthropogenic emissions (Blando and Turpin, 2000). Because EC only originates from primary emissions and is inert in the atmosphere, it is often used as a marker to estimate POC concentration in the atmosphere (Turpin and Huntzicker, 1991). By this approach, the concentrations of SOC and POC can be evaluated from the

following equations (Turpin and Huntzicker, 1995; Strader et al., 1999; Castro et al., 1999; Chu, 2005; Yu et al., 2009; Day et al., 2015):

$$POC = (OC/EC)_{min} \times EC \quad (1)$$

$$SOC = OC_{total} - POC \quad (2)$$

The $(OC/EC)_{min}$ ratios were the minimum OC/EC ratios calculated at each sampling height, and OC_{total} were the mass concentrations of OC. The concentration of POC calculated using the first equation means the primary carbonaceous aerosols from fossil fuel combustion (Turpin and Huntzicker, 1995). In this study, the $(OC/EC)_{min}$ ratios were 5.0, 2.6 and 2.5 at the ground level, 120 m and 260 m, respectively. POC showed the largest mass concentration at the ground level (4.7 ± 2.3 μg m^{-3}), while SOC were more abundant at 120 m (5.1 ± 2.9 μg m^{-3}) and 260 m (4.7 ± 2.2 μg m^{-3}) (Table 1). The SOC/POC ratios at 120 m (1.8 ± 0.79) and 260 m (1.9 ± 0.92) were higher than those at the ground level (0.51 ± 0.3) (Table. S1), demonstrating that more aged aerosols accumulated at upper layers (Fig. 2f).

3.2 Organic molecular characterization

Table 2 shows the concentration ranges of dicarboxylic acids, oxoacids and α-dicarbonyls with the mean values. Mean concentrations of total diacids at 120 m (370 ± 255 ng m^{-3}) and 260 m (380 ± 216 ng m^{-3}) were almost the same, which were larger than that at the ground level (285 ± 143 ng m^{-3}). Meanwhile, the relative abundances of total diacids in carbonaceous fractions (organic carbon and total carbon) reached maximum values at 260 m (Table S1). Such vertical phenomena were also observed for total oxoacids and α-dicarbonyls, suggesting that the aging level of diacids and related compounds slightly increased at 260 m in the urban troposphere.

The molecular distributions of dicarboxylic acids were characterized by the dominance of oxalic acid (C_2), followed by malonic (C_3) and succinic (C_4) acids (Fig. 4). Their concentrations were higher at upper layers (Figs. S3h − j) with similar diurnal trends (Figs. S3a – c), illustrating C_2, C_3 and C_4 diacids derived from common primary sources and/or secondary oxidation pathways. C_3 diacid is mainly formed via hydrogen abstraction of OH radicals on C_4 diacid, followed by the

decarboxylation reaction (Kawamura and Ikushima, 1993). The mass concentration ratio of malonic acid to succinic acid is a useful marker to estimate the relative contribution of primary production and photochemical formation to organic aerosols. The C_3/C_4 ratio shows a characteristically lower value for primary emissions (e.g., vehicular exhausts: 0.25 − 0.44) (Kawamura and Ikushima, 1993), whereas it has a larger value more than or equal to unity in aged aerosol (Kawamura and Sakaguchi, 1999). In this paper, the mean C_3/C_4 ratio values at 260 m (1.2 ± 0.21) were slightly larger than those at ground surface (1.1 ± 0.2) and 120 m (1.1 ± 0.14) (Table S1), implying that organic aerosols at 260 m were influenced by photochemical formation via regional transport.

Adipic acid (C_6), the major oxidation product of 2-methylglutaric (iC_6) from anthropogenic cyclic olefins (Hamilton et al., 2006; Müller et al., 2007) and intermediate of relatively long-chain diacids, was more abundant at upper heights, especially at 260 m (Fig. 4). Good correlations were observed for C_6/iC_6 with C_6/total diacids at the ground level ($r_1^2 = 0.66$) and 260 m ($r_3^2 = 0.94$) (Fig. S4a), which indicated that the photooxidation of cyclic olefins from anthropogenic sources is an important contributor to adipic acid in Beijing. Azelaic acid (C_9) is a major oxidation product of unsaturated fatty acids (Matsunaga et al., 1999) from meal cooking (Rogge et al., 1991) (Stephanou and Stratigakis, 1993), biomass burning (Ballentine et al., 1998), marine plankton activities (Mochida et al., 2007) and terrestrial higher plants emissions (Ballentine et al., 1998). Meanwhile, Kawamura and Kaplan (1987) reported that vehicular emission is also an important source to azelaic acid. The relative abundance of C_9 in total diacids (C_9/total diacids) showed the largest value (0.07 ± 0.02) at the ground level (Table S1), implying that C_9 may be derived from the photooxidation of corresponding hydrocarbons from local vehicular emissions. Positive linear correlations were found between C_6/C_9 and C_6/total diacids at 120 m ($r_2^2 = 0.51$) and 260 m ($r_3^2 = 0.86$) (Fig. S4b), suggesting that the breakdown of C_9 carbon chain to form C_6 may enhance during its upward transport.

Phthalic acid (Ph) was the fourth abundant diacid in this study (Fig. 4), which can be emitted from motor vehicles and fossil fuel combustion or secondarily oxidized from aromatic hydrocarbons like naphthalene from coal and biofuel combustions (Kautzman et al., 2010; Wang et al., 2006a). Mass concentrations of Ph decreased with the sampling heights, illustrating that vehicular exhausts at the ground level was a major source to phthalic acid. Terephthalic acid (tPh), an isomer of Ph, is a

tracer of plastic burning in municipal wastes (Fu et al., 2010; Kawamura and Pavuluri, 2010; Simoneit et al., 2005). Contrary to the vertical distribution of Ph, the average concentration of tPh at the ground level (12 ± 10 ng m^{-3}) was slightly lower than those at 120 m (15 ± 15 ng m^{-3}) and 260 m (13 ± 11 ng m^{-3}).

Oxocarboxylic acids, the intermediates of the oxidation of mono-carboxylic acids, can further be photochemically oxidized to form diacids (Warneck, 2003; Carlton et al., 2007). The glyoxylic acid (ωC_2) is the dominant oxoacid, followed by pyruvic acid (Pyr) (Fig. 4). Both acids were more abundant at upper layers. Concentrations of total dicarbonyls varied from 1.8 ng m^{-3} to 33 ng m^{-3} with a maximum value (10 ± 7.4 ng m^{-3}) at 260 m. Glyoxal (Gly) and methyglyoxal (MeGly), the two smallest α-dicarbonyls, are mainly produced by the photooxidation of biogenic (Zimmermann and Poppe, 1996; Fick et al., 2004; Ervens et al., 2004) (e.g., isoprene and monoterpenes) and anthropogenic (Volkamer et al., 2001) (e.g., aromatics, acetone and acetylene) volatile organic compounds (VOCs). And both are important precursors to form less-volatile organic acids such as ωC_2, Pyr (Lim et al., 2005). Concentrations of Gly and MeGly increased with the sampling heights, and their concentration variations were similar to those of ωC_2 and Pyr (Figs. S3d − g), illustrating that ωC_2, Pyr and α-dicarbonyls had similar sources and/or formation pathways.

3.3 Restriction versus non-restriction periods

Owing to the regional scale of haze events in China, the Chinese government took measures to cut down anthropogenic emissions in Beijing and surrounding areas to ensure good air quality during the 2015 Victory Parade period. These strict restrictions included the stopping construction and demolition activities, banning vehicles with odd and even plate numbers on alternate days, forbidding open burnings and shutting down factories and power plants in Tianjin City, Inner Mongolia Autonomous Region, Hebei, Shandong, Shanxi and Henan provinces. The restriction time (R) started from 20th August to 3rd September 2015. Before and after this period were defined as the first (N1) and second (N2) non-restriction periods, respectively. The concentration ratios of selected organic compounds during the restriction to non-restriction periods (R/N) were calculated (Fig. S5). The ratio less than unity indicates that the control on the air quality effectively improves in Beijing. Both the primary incomplete combustion sources and the wind are two key influential factors (Liang et al., 2017; Xu et al.,

2017). In this study, the R/N ratios of OC, EC, POC, total diacids, total oxoacids and dicarbonyls were lower than unity, but their R/N2 ratios were larger than corresponding R/N1 values (Fig. S5). These results showed that the improvement of air quality in Beijing was mainly influenced by the control on anthropogenic emissions, followed by the wind (Liang et al., 2017; Xu et al., 2017). The lower concentrations of organic compounds in the second non-restriction period than those in the first non-restriction period were attributed to the more influence of clean northwesterly winds (Fig. S1a). The R/N ratios for OC/EC and SOC/POC were larger than or equal to unit due to the reduction of primary pollutants from incomplete burning activities under control measurements. Moreover, both R/N1 and R/N2 ratios for SOC/POC decreased with the sampling heights, demonstrating that vehicular emissions at the ground level was an important factor to dicarboxylic acids. The reduction of vehicular emissions resulted in the relatively low concentration of POC and the highest SOC/POC ratio at the ground level in restriction period. The contribution of vehicular emissions to upper sampling layers decreased during the atmospheric upward transport.

Footprint regions of atmospheric particles are shown in Fig. 5. During the non-restriction periods, Beijing was dominated by regional transport from the south and southwest industrial areas. However, the footprint area of organic aerosols in restriction period was mainly located in the northeastern direction of Beijing, where was relatively clean. Combined with the wind field, the wind speeds and directions at the ground level showed little difference in the whole sampling time (Fig. S1a). The wind direction at 120 m was similar to that at 260 m in each non-restriction period, but wind speeds at 260 m were larger than those at 120 m. In comparison to the second non-restriction period, the organic aerosols at 120 m and 260 m were mainly affected by southwesterly wind in the first non-restriction episode. As for the restriction period in Beijing, more clean air masses from the northern areas arrived at 120 m, while organic aerosols at 260 m were largely influenced by the northwesterly wind and accompanied by the influence of polluted southerly and southeasterly winds. Photochemical production of diacids and related compounds can occur in the atmospheric long-range transport.

Similarly, the R/N ratios for most diacids and related compounds were lower than unity (Fig. 6), especially for ωC_2, Pyr, tPh and α-dicarbonyls. Owing to the influence of wind, the decreased level of main diacids, oxoacids and α-dicabonyls (20% −

69%) were stronger during the first non-restriction period than that (10% − 55%) in the second non-restriction period. These phenomena indicated that anthropogenic emissions largely contributed to diacids and related organic precursors in Beijing. Furthermore, the decreased orders of most diacids and related compounds were the ground level < 120 m < 260 m in restriction period compared to the non-restriction periods (Table S2). This also supported the conclusion that a upward transport of vehicular emissions was existed, and organic aerosols at upper layers were more attributed to regional transport.

3.4 Possible formation pathways of organic acids

To better estimate the relative contribution of primary sources and photochemical transformation to diacids and related compounds, linear regression analyses for selected marker compounds (Fig. S2) and diagnostic ratios (Fig. 7) were employed in this study. Levoglucosan is an important tracer of biomass burning (Simoneit, 2002). The isoprene SOA tracers are the sum of six oxidation products of isoprene, including 2-methylglyceric acid, C_5-alkene triols (*cis*-2-methyl-1,3,4-trihydroxy-1-butane, *trans*-2-methyl-1,3,4-trihydroxy-1-butene and 3-methyl-2,3,4-trihydroxy-1-butane), 2-methylthreitol and 2-methylerythritol (Claeys et al., 2004; Fan et al., 2020). Isoprene, the major biogenic volatile organic compound, is abundantly derived from plants emissions (Sharkey et al., 2007). Compared to total α-dicarbonyls, better correlations were found between isoprene SOA tracers and total diacids ($0.35 \leq r^2 \leq 0.46$) and oxoacids ($0.32 \leq r^2 \leq 0.48$), indicating that higher plants emissions contribute to diacids and related compounds to a certain extent in summer in Beijing. Levoglucosan only correlated well with total diacids ($r_2^2 = 0.51$, $r_3^2 = 0.41$), oxoacids ($r_2^2 = 0.53$, $r_3^2 = 0.43$) and α-dicarbonyls ($r_2^2 = 0.63$, $r_3^2 = 0.52$) at upper heights, demonstrating that biomass burning was a key source to organic aerosols.

The concentration ratio of relative abundance of C_2 in total diacids (C_2/total diacids) is known as a useful marker to assess the photochemical processing level, because C_2 is the end product mostly formed via the oxidation of longer carbon-chain diacids and other precursors in the atmosphere (Kawamura and Bikkina, 2016). The C_2/total diacids ratio enhanced with the increase of C_2-C/TC ($0.75 \leq r^2 \leq 0.8$), C_2/C_3 ($0.58 \leq r^2 \leq 0.8$) and C_2/C_4 ($0.26 \leq r^2 \leq 0.62$) ratios (Figs. 7a, c − d), suggesting a possible formation of oxalic acid from higher carbon number homologues and related compounds. However, there was no

relationship between (C_3–C_{12})-C/TC and C_2/total diacids, which imply that the supply of longer-chain diacids may be faster than their degradation rates to produce oxalic acid in Beijing. Intermediate diacids can still be abundantly produced by oxidation of organic precursors during the atmospheric long-range transport. Meanwhile, C_4/total diacids ratio exhibited positive correlations with the C_4/C_5 ($0.28 \leq r^2 \leq 0.41$) and C_4/C_6 ($0.24 \leq r^2 \leq 0.48$) ratios (Figs. 7e − f), illustrating that glutaric and adipic acids may possibly photodegrade to form succinic acid. These results suggested that the photodegradation of longer chain diacids contributed to the formation of lower diacids homologues after primary emissions, such as biomass burning and vehicular emissions in Beijing.

The 325-m meteorological tower in Beijing is well equipped for the investigation of the vertical structure of urban boundary layer (UBL) and the mixing mechanism of organic aerosols among the UBL. Guo et al. (2016) found that the UBL often has a significant thermal stratification in heavy haze periods, which shows the convective instability in daytime and the extreme convective stability in nighttime. Meanwhile, the geometric parameters of wind speed vector and the efficiency of turbulent transport also show more obvious diurnal variations. Concentrations of organic compounds are significantly affected by the combined effect of source intensity, meteorological condition, and vertical structure of UBL.

Based on the sampling records, 16 − 17 August, 29 − 30 August, and 7 − 8 September were labeled as polluted episodes. The pollution level was defined by the air quality index (AQI) according to local reports from the environmental monitor station. Previous studies reported that the photochemical oxidation of biogenic and anthropogenic VOCs results in semi-volatile gaseous Gly and MeGly, which can partition into the aerosol phase enriched with liquid water content or cloud/fog droplets (Volkamer et al., 2001; Zimmermann and Poppe, 1996; Fick et al., 2004; Ervens et al., 2004). In these transformations, C_2 is an end product formed via photochemical oxidation of the key intermediates such as ωC_2 and Pyr (Lim et al., 2005). Thus, the ratios of $C_2/\omega C_2$, C_2/Pyr, C_2/Gly and C_2/MeGly were applied to better understand the aqueous oxidation mechanism of organic matters.

Compared to clean days, the relatively strong aqueous-phase oxidation of related precursors (ωC_2, Pyr, Gly and MeGly) contributed to the accumulation of C_2 in polluted days. Positive correlations were noteworthy for C_2/total diacids with

C_2/Gly ($0.42 \leq r^2 \leq 0.58$) and C_2/MeGly ($0.53 \leq r^2 \leq 0.65$) at three sampling heights, while good linear relationships for C_2/total diacids with $C_2/\omega C_2$ ($r_1^2 = 0.58$) and C_2/Pyr ($r_1^2 = 0.5$) only existed at the ground level in polluted episodes (Fig. 8). In contrast, no significant connections were found between relative abundance of C_2 in total diacids and its mass ratios with four precursors in clean days. Therefore, the increased aqueous-phase oxidation may be a major source of oxalic acid. It is worth noting that OH radical-initiated aqueous oxidation may dominate the production of secondary organic aerosol in polluted days. The aqueous formation in cloud or wet aerosol is also an important pathway to diacids and related compounds (Carlton et al., 2006; Carlton et al., 2007; Ervens and Volkamer, 2010; Tan et al., 2010).

Aged organic aerosols are usually characterized by the larger contribution of oxalic acid to WSOC (C_2-C/WSOC). For example, C_2-C/WSOC ratio was higher in the photochemically aged aerosols collected at Hong Kong (6.8%) (Ho et al., 2011) and Mount Hua (6.3%) (Meng et al., 2014) compared with the ratio (0.17%) in Ulaanbaatar aerosols that are significantly affected by substantial anthropogenic emissions (Jung et al., 2010). Due to the high temperature and relative humidity, the photochemical reaction is active in Hong Kong (Ho et al., 2011). Mount Hua is the highest mountain in central China and is a typically isolated site to investigate the atmospheric long-range transport of organic compounds (Meng et al., 2014). In contrast, diacids and related compounds in winter were mainly associated with uncontrolled wastes plastic burning, coal power plants and vehicular emissions in Ulaanbaatar (Jung et al., 2010). Generally, in clean days, the C_2-C/WSOC ratio showed relatively large values at upper heights in this study (Fig. 9a). Moreover, in the transition from clean to polluted days, the C_2-C/WSOC ratio values at the ground level, 120 m and 260 m slightly increased.

However, in the more polluted days, C_2-C/WSOC ratios at the ground level were obviously higher than those at 120 m and 260 m owing to the accumulation of pollutants and moisture in ground surface atmosphere (Guinot et al., 2006). In comparison to the moderately polluted events of 17th August (P1) and 8th September (P3), C_2-C/WSOC ratio maximized at 120 m (3.2%) in lightly polluted day of 29th August (P2). According to the concentrations of OC and EC, the strongest polluted event occurred on 8th September during the field campaign in Beijing. The C_2-C/WSOC ratio at the ground level in P3 (5.3%) was higher than that in P1 (4.7%), which may increase with an enhancement of the pollution. Furthermore,

C_2-C/WSOC ratio was larger in the ground level (5.3%) followed by 120 m (2.4%) and 260 m (2.2%) in P3, demonstrating that C_2-C/WSOC ratio may decrease with an increase of sampling heights. These phenomena may indicate that the moderately polluted days were favorable for aqueous formation of C_2 in the lower troposphere, especially at the ground level. Similarly, the C_2-C/OC ratios at three sampling layers were higher in polluted days than clean days in general (Fig. 9b). We observed largest values of C_2-C/OC at higher levels of 120 m and 260 m, which may be caused by more accumulation of POC from local anthropogenic emissions at the ground level (Fig. 2).

Different from the vertical distribution of C_2-C/WSOC ratios, the largest value of Ph-C/WSOC was mostly observed at the ground level (0.70%), followed by 120 m (0.53%) and 260 m (0.45%) (Fig. 9c). In comparison to the ratio value in P2, the large differences between Ph-C/WSOC ratio at the ground level and upper layers (≥ 0.6%) in P1 and P3 also supported the stagnant meteorological condition in the moderately polluted days. But the value of Ph-C/OC ratio at the ground level in polluted days were lower than those in clean days (Fig. 9d), which may be caused by the accumulation of organic precursors, like naphthalene. Unlike gas pollutants, high loadings of fine aerosol interact strongly with meteorological variables in the planetary boundary layer (PBL). Both aerosol scattering and absorption reduce the amount of solar radiation reaching the ground and thus reduce the sensible heat fluxes, which suppresses the development of PBL and further aggravate the pollution level (Li et al., 2017). Such positive feedback is especially strong in heavy pollution events (Li et al., 2017), hence the photochemical formation of Ph at the ground level may be not as effective as clean days.

Hydrated Gly and MeGly formed via the photooxidations of biogenic and anthropogenic VOCs can subsequently produce ωC_2 and Pyr, and ultimately generate C_2 (Ervens et al., 2004; Lim et al., 2005). In P1, only ωC_2-C/WSOC ratio at the ground level remarkably increased (Fig. 9g). But all the ratios of Pyr-C/WSOC, ωC_2-C/WSOC, Gly-C/WSOC and MeGly-C/WSOC were obviously larger at the ground level than those at upper layers in P3 (Figs. 9e, i, k). These results suggested that aqueous oxidation pathway was an important factor to the formation of C_2, Pyr, ωC_2 and α-dicarbonyls in the more polluted days. The ratios of C_2-C/WSOC, Pyr-C/WSOC, ωC_2-C/WSOC, Gly-C/WSOC and MeGly-C/WSOC at three sampling levels in transformation periods were divided by those in the moderately polluted days (P/T) to evaluate the importance of aqueous

formation. The transformation periods were defined as the day before haze days. The P1/T1 ratios of C_2-C/WSOC, Pyr-C/WSOC, ωC_2-C/WSOC, Gly-C/WSOC and MeGly-C/WSOC were lower than corresponding P3/T3 ratios (Table. S3), implying that during the strongest polluted event in this study, aqueous formation may contribute more to the concentrations of C_2, Pyr, ωC_2, Gly and MeGly. In addition, orders of P3/T3 ratio all values were: ground level > 120 m > 260 m. The vertical P3/T3 ratios for ωC_2-C/WSOC (the ground level: 5.2, 120 m: 1.8, 260 m: 1.4), Gly-C/WSOC (the ground level: 5.7, 120 m: 1.8, 260 m: 1.6) and MeGly-C/WSOC (the ground level: 5.8, 120 m: 2.0, 260 m: 1.5) were higher than those of C_2-C/WSOC and Pyr-C/WSOC. These phenomena implied that the aqueous formation of C_2, Pyr, ωC_2 and α-dicarbonyls may decrease with the sampling heights in the most polluted events. And the increasing level of aqueous formation of C_2 and related precursors may be associated with the pollution strength in Beijing.

3.5 Source apportionment of organic acids using PMF analysis

Based on the data of organic tracers and ions, the positive matrix factorization (PMF, USEPA) was employed to estimate the relative contributions of primary sources and secondary formation pathways to diacids and related compounds in this study. The abundance, naming abbreviations and indicative sources of the tracer compounds were summarized in Table 3. Details of model stability of the six-factor solution was provided in Table S4. The PMF-resolved source profiles for the six factors were shown in Figs. 10a − f. Each factor was identified according to the dominant species. Secondary sulfate formation was identified by SO_4^{2-} and isoprene SOA tracers, which indicated ozonolysis, OH radical-initiated oxidation and aqueous processing. Secondary nitrate formation was identified by the dominance of NO_3^- and isoprene SOA tracers, mainly representing the OH radical-initiated oxidation. Owing to the existence of two double bonds, isoprene is highly reactive and is readily oxidized in the atmosphere by OH, NO_3 and O_3. Higher loading of the isoprene SOA tracers was observed in the factor of secondary sulfate formation than secondary nitrate formation, which may indicate more overlapping of oxidation pathways.

Meanwhile, in comparison to NO_3^- ($r^2 \leq 0.23$), better correlations were found between isoprene SOA tracers and SO_4^{2-} ($0.44 \leq r^2 \leq 0.67$) (Fig. S6), being consistent with the above conclusion. Biomass burning was identified by the dominant species

of levoglucosan and EC. Contributions of vehicle exhausts were identified by the dominance of hopanes (*αβ*-hopane, *αβS&R*-homohopane and *αβS&R*-bishomohopane) and EC. Plants emissions were identified by the dominance of isoprene SOA tracers. Because the isoprene SOA tracers are not only viewed as a representative of SOA tracers (Magda et al., 2004;Surratt et al., 2010) but also a marker of biogenic sources (Guenther et al., 2006), like terrestrial higher plants emissions (Sharkey et al., 2007). Coal combustion was identified by dominant species of the PAHs with their molecular weights of 276 (indeno-[1,2,3-*cd*]pyrene and benzo [*ghi*]perylene) and hopanes.

The PMF-resolved factor contributions to total species, and total diacids, oxoacids and α-dicarbonyls were shown in Fig. 10g − j. The secondary source (secondary sulfate formation and secondary nitrate formation) was the dominant contributor (44%) to total species, followed by biomass burning (27%) and motor vehicles (14%). Similar factor distribution was also observed for total diacids, oxoacids and α-dicarbonyls, but the contribution of motor vehicles enhanced, especially in total oxoacids. The plant emission is a small contributor (5 − 8%) to organic compounds. In this study, the contributed fraction of anthropogenic emissions (49 − 55%), including biomass burning, motor vehicles and coal combustion (Zhu et al., 2018), to diacids and related compounds were slightly larger than that of secondary formation pathways (37 − 44%).

4. Conclusions

Current knowledge on vertical distributions of dicarboxylic acids and related compounds in fine aerosol collected in the urban boundary layer is very limited. Compared to the ground measurements, the vertical studies can provide special insights into the photochemical mechanisms and regional transport of organic aerosols. In this study, being different from the vertical distribution of phthalic acid, the main organic acids generally showed higher values at 260 m and 120 m than those at the ground surface. Thus, diacids and related compounds were influenced by both vehicular emissions at the ground level, whereas the atmospheric long-range transport was also an important contributor to organic compounds in the urban troposphere. Unlike clean days, the relative contribution of aqueous formation to dicarboxylic acids enhanced in polluted days, especially at the ground level. Moreover, the increasing level of aqueous formation of C_2 and related precursors may be associated with the pollution strength in Beijing. Combined with the influence of wind, mass concentrations of total diacids,

oxoacids and α-dicarbonyls were largely cut down (22 – 58%) under the control on anthropogenic emissions. Here, the PMF results showed that the contributed fraction of anthropogenic emissions (49 − 55%) to diacids and related compounds such as biomass burning, motor vehicles and coal combustion (Zhu et al., 2018) were more significant than that of secondary formation pathways (37 − 44%).

Data availability. The dataset for this paper is available upon request from the corresponding author (fupingqing@tju.edu.cn).

Competing interests. The authors declare that they have no conflict of interest.

Author contributions. Pingqing Fu designed this research. $PM_{2.5}$ samples were collected by Hong Ren. Laboratory analyses were performed by Wanyu Zhao and Hong Ren. The manuscript was written by Wanyu Zhao and Pingqing Fu with consultation from all other authors.

Acknowledgments and Data

This work was supported the National Natural Science Foundation of China (Grant Nos. 41625014 and 41961130384). The authors declare no competing financial interests. Supporting description of analyzing methods, figures and tables are provided in the supporting information. The data used in this manuscript are listed in the tables, figures, and supplementary materials.

References

Andreae, M., and Rosenfeld, D.: Aerosol–cloud–precipitation interactions. Part 1. The nature and sources of cloud-active aerosols, Earth-Sci. Rev., 89, 13-41, https://doi.org/10.1016/j.earscirev.2008.03.001, 2008.

Andreae, M. O., Artaxo, P., Beck, V., Bela, M., Freitas, S., Gerbig, C., Longo, K., Munger, J. W., Wiedemann, K. T., and Wofsy, S. C.: Carbon monoxide and related trace gases and aerosols over the Amazon Basin during the wet and dry seasons, Atmos. Chem. Phys., 12, 6041-6065, doi: 10.5194/acp-12-6041-2012, 2012.

Andreae, M. O., Acevedo, O. C., Araùjo, A., Artaxo, P., Barbosa, C. G. G., Barbosa, H. M. J., Brito, J., Carbone, S., Chi, X., Cintra, B. B. L., da Silva, N. F., Dias, N. L., Dias-Júnior, C. Q., Ditas, F., Ditz, R., Godoi, A. F. L., Godoi, R. H. M., Heimann, M., Hoffmann, T., Kesselmeier, J., Könemann, T., Krüger, M. L., Lavric, J. V., Manzi, A. O., Lopes, A. P., Martins, D. L., Mikhailov, E. F., Moran-Zuloaga, D., Nelson, B. W., Nölscher, A. C., Santos Nogueira, D., Piedade, M. T. F., Pöhlker, C., Pöschl, U., Quesada, C. A., Rizzo, L. V., Ro, C. U., Ruckteschler, N., Sá, L. D. A., de Oliveira Sá, M., Sales, C. B., dos Santos, R. M. N., Saturno, J., Schöngart, J., Sörgel, M., de Souza, C. M., de Souza, R. A. F., Su, H., Targhetta, N., Tóta, J., Trebs, I., Trumbore, S., van Eijck, A., Walter, D., Wang, Z., Weber, B., Williams, J., Winderlich, J., Wittmann, F., Wolff, S., and Yáñez-Serrano, A. M.: The Amazon Tall Tower Observatory (ATTO): overview of pilot measurements on ecosystem ecology, meteorology, trace gases, and aerosols, Atmos. Chem. Phys., 15, 10723-10776, doi: 10.5194/acp-15-10723-2015,

2015.

Ballentine, D. C., Macko, S. A., and Turekian, V. C.: Variability of stable carbon isotopic compositions in individual fatty acids from combustion of C_4 and C_3 plants: implications for biomass burning, Chem. Geol., 152, 151-161, https://doi.org/10.1016/S0009-2541(98)00103-X, 1998.

Bilde, M., Barsanti, K., Booth, M., Cappa, C. D., Donahue, N. M., Emanuelsson, E. U., McFiggans, G., Krieger, U. K., Marcolli, C., Topping, D., Ziemann, P., Barley, M., Clegg, S., Dennis-Smither, B., Hallquist, M., Hallquist, Å. M., Khlystov, A., Kulmala, M., Mogensen, D., Percival, C. J., Pope, F., Reid, J. P., Ribeiro da Silva, M. A. V., Rosenoern, T., Salo, K., Soonsin, V. P., Yli-Juuti, T., Prisle, N. L., Pagels, J., Rarey, J., Zardini, A. A., and Riipinen, I.: Saturation vapor pressures and transition enthalpies of low-volatility organic molecules of atmospheric relevance: From dicarboxylic acids to complex mixtures, Chem. Rev., 115, 4115-4156, doi: 10.1021/cr5005502, 2015.

Blando, J. D., and Turpin, B. J.: Secondary organic aerosol formation in cloud and fog droplets: a literature evaluation of plausibility, Atmos. Environ., 34, 1623-1632, 2000.

Bond, T. C., Doherty, S. J., Fahey, D. W., Forster, P. M., Berntsen, T., DeAngelo, B. J., Flanner, M. G., Ghan, S., Kärcher, B., Koch, D., Kinne, S., Kondo, Y., Quinn, P. K., Sarofim, M. C., Schultz, M. G., Schulz, M., Venkataraman, C., Zhang, H., Zhang, S., Bellouin, N., Guttikunda, S. K., Hopke, P. K., Jacobson, M. Z., Kaiser, J. W., Klimont, Z., Lohmann, U., Schwarz, J. P., Shindell, D., Storelvmo, T., Warren, S. G., and Zender, C. S.: Bounding the role of black carbon in the climate system: A scientific assessment, J. Geophys. Res. Atmos., 118, 5380-5552, doi:10.1002/jgrd.50171, 2013.

Brioude, J., Arnold, D., Stohl, A., Cassiani, M., Morton, D., Seibert, P., Angevine, W., Evan, S., Dingwell, A., Fast, J. D., Easter, R. C., Pisso, I., Burkhart, J., and Wotawa, G.: The Lagrangian particle dispersion model FLEXPART-WRF version 3.1, Geosci. Model Dev., 6, 1889-1904, doi: 10.5194/gmd-6-1889-2013, 2013.

Carlton, A. G., Turpin, B. J., Lim, H. J., Altieri, K. E., and Seitzinger, S.: Link between isoprene and secondary organic aerosol (SOA): Pyruvic acid oxidation yields low volatility organic acids in clouds, Geophys. Res. Lett., 33, 272-288, https://doi.org/10.1029/2005GL025374, 2006.

Carlton, A. G., Turpin, B. J., Altieri, K. E., Seitzinger, S., Reff, A., Lim, H.-J., and Ervens, B.: Atmospheric oxalic acid and SOA production from glyoxal: Results of aqueous photooxidation experiments, Atmos. Environ., 41, 7588-7602, https://doi.org/10.1016/j.atmosenv.2007.05.035, 2007.

Castro, L. M., Pio, C. A., Harrison, R. M., and Smith, D. J. T.: Carbonaceous aerosol in urban and rural European atmospheres: estimation of secondary organic carbon concentrations, Atmos. Environ., 33, 2771-2781, https://doi.org/10.1016/S1352-2310(98)00331-8, 1999.

Chi, X., Winderlich, J., Mayer, J. C., Panov, A. V., Heimann, M., Birmili, W., Heintzenberg, J., Cheng, Y., and Andreae, M. O.: Long-term measurements of aerosol and carbon monoxide at the ZOTTO tall tower to characterize polluted and pristine air in the Siberian taiga, Atmos. Chem. Phys., 13, 12271-12298, doi: 10.5194/acp-13-12271-2013, 2013.

Chow, J., Watson, J., Chen, L.-W., Paredes-Miranda, G., Chang, M.-C., Trimble, D., Fung, K., Zhang, H., and Zhen Yu, J.: Refining temperature measures in thermal/optical carbon analysis, Atmos. Chem. Phys., 5, 2961-2972, 2005.

Chu, S.-H.: Stable estimate of primary OC/EC ratios in the EC tracer method, Atmos. Environ., 39, 1383-1392, https://doi.org/10.1016/j.atmosenv.2004.11.038, 2005.

Claeys, M., Graham, B., Vas, G., Wang, W., Vermeylen, R., Pashynska, V., Cafmeyer, J., Guyon, P., Andreae, M. O., Artaxo, P., and Maenhaut, W.: Formation of secondary organic aerosols through photooxidation of isoprene, Science, 303, 1173, doi:

10.1126/science.1092805, 2004.

Clarke, A. D., Shinozuka, Y., Kapustin, V. N., Howell, S., Huebert, B., Doherty, S., Anderson, T., Covert, D., Anderson, J., and Hua, X.: Size distributions and mixtures of dust and black carbon aerosol in Asian outflow: Physiochemistry and optical properties, Journal of Geophysical Research Atmospheres, 35, 1217-1226, 2004.

Cong, Z., Kawamura, K., Kang, S., and Fu, P.: Penetration of biomass-burning emissions from South Asia through the Himalayas: new insights from atmospheric organic acids, Scientific Reports, 5, doi:10.1038/srep09580, 2015.

Day, M. C., Zhang, M., and Pandis, S. N.: Evaluation of the ability of the EC tracer method to estimate secondary organic carbon, Atmos. Environ., 112, 317-325, https://doi.org/10.1016/j.atmosenv.2015.04.044, 2015.

Desyaterik, Y., Sun, Y., Shen, X., Lee, T., Wang, X., Wang, T., and Jr, J. L. C.: Speciation of "brown" carbon in cloud water impacted by agricultural biomass burning in eastern China, J. Geophys. Res. Atmos., 118, 7389-7399, doi: 10.1002/jgrd.50561, 2013.

Drozd, G., Woo, J., Häkkinen, S. A. K., Nenes, A., and McNeill, V. F.: Inorganic salts interact with oxalic acid in submicron particles to form material with low hygroscopicity and volatility, Atmos. Chem. Phys., 14, 5205-5215, doi: 10.5194/acp-14-5205-2014, 2014.

Ervens, B., Feingold, G., Frost, G. J., and Kreidenweis, S. M.: A modeling study of aqueous production of dicarboxylic acids: 1. Chemical pathways and speciated organic mass production, J. Geophys. Res. Atmos., 109, https://doi.org/10.1029/2003JD004387, 2004.

Ervens, B., and Volkamer, R.: Glyoxal processing by aerosol multiphase chemistry: towards a kinetic modeling framework of secondary organic aerosol formation in aqueous particles, Atmos. Chem. Phys., 10, 12371-12431, https://doi.org/10.5194/acp-10-8219-2010, 2010.

Falkovich, A., Graber, E., Schkolnik, G., Rudich, Y., Maenhaut, W., and Artaxo, P.: Low molecular weight organic acids in aerosol particles from Rondonia, Brazil, during the biomass-burning, transition and wet periods, Atmos. Chem. Phys., 5, 781-797, 2005.

Fan, Y. B., Liu, C. Q., Li, L. J., Ren, L. J., Ren, H., Zhang, Z. M., Li, Q. K., Wang, S., Hu, W., Deng, J. J., Wu, L. B., Zhong, S. J., Zhao, Y., Pavuluri, C. M., Li, X. D., Pan, X. L., Sun, Y. L., Wang, Z. F., Kawamura, K., Shi, Z. B., and Fu, P. Q.: Large contributions of biogenic and anthropogenic sources to fine organic aerosols in Tianjin, North China, Atmos. Chem. Phys., 20 (1), 117-137, 2020.

Fick, J., Nilsson, C., and Andersson, B.: Formation of oxidation products in a ventilation system, Atmos. Environ., 38, 5895-5899, https://doi.org/10.1016/j.atmosenv.2004.08.020, 2004.

Fu, P. Q., Kawamura, K., Pavuluri, C. M., Swaminathan, T., and Chen, J.: Molecular characterization of urban organic aerosol in tropical India: contributions of primary emissions and secondary photooxidation, Atmos. Chem. Phys., 10, 2663-2689, 2010.

Fu, P., Kawamura, K., Chen, J., Li, J., Sun, Y., Liu, Y., Tachibana, E., Aggarwal, S., Okuzawa, K., and Tanimoto, H.: Diurnal variations of organic molecular tracers and stable carbon isotopic composition in atmospheric aerosols over Mt. Tai in the North China Plain: an influence of biomass burning, Atmos. Chem. Phys., 12, 8359-8375, 2012.

Fu, P. Q., Kawamura, K., Usukura, K., and Miura, K.: Dicarboxylic acids, ketocarboxylic acids and glyoxal in the marine aerosols collected during a round-the-world cruise, Marine Chemistry, 148, 22-32, 10.1016/j.marchem.2012.11.002, 2013a.

Fu, P., Kawamura, K., Chen, J., Charrière, B., and Sempéré, R.: Organic molecular composition of marine aerosols over the Arctic ocean in summer: contributions of primary emission and secondary aerosol formation, Biogeosciences, 10(2), 653–667, doi:10.5194/bg-10-653-2013, 2013b.

Graham, B., Mayol-Bracero, O. L., Guyon, P., Roberts, G. C., Decesari, S., Facchini, M. C., Artaxo, P., Maenhaut, W., Köll, P., and Andreae, M. O.: Water-soluble organic compounds in biomass burning aerosols over Amazonia 1. Characterization by NMR and GC-MS, J. Geophys. Res. Atmos., 107, doi:10.1029/2001JD000336, 2002.

Guenther, A., Karl, T., Harley, P., Wiedinmyer, C., Palmer, P. I., and Geron, C.: Estimates of global terrestrial isoprene emissions using MEGAN (Model of Emissions of Gases and Aerosols from Nature), Atmos. Chem. Phys., 6, 3181-3210, 10.5194/acp-6-3181-2006, 2006.

Guinot, B., Roger, J.-C., Cachier, H., Pucai, W., Jianhui, B., and Tong, Y.: Impact of vertical atmospheric structure on Beijing aerosol distribution, Atmos. Environ., 40, 5167-5180, https://doi.org/10.1016/j.atmosenv.2006.03.051, 2006.

Guo, X., Sun, Y., and Miao, S.: Characterizing urban turbulence under haze pollution: Insights into temperature–humidity dissimilarity, Boundary-Layer Meteorology, 158, 501-510, doi: 10.1007/s10546-015-0104-y, 2016.

Hallquist, M., Wenger, J. C., Baltensperger, U., Rudich, Y., Simpson, D., Claeys, M., Dommen, J., Donahue, N. M., George, C., Goldstein, A. H., Hamilton, J. F., Herrmann, H., Hoffmann, T., Iinuma, Y., Jang, M., Jenkin, M. E., Jimenez, J. L., Kiendler-Scharr, A., Maenhaut, W., McFiggans, G., Mentel, T. F., Monod, A., Prévôt, A. S. H., Seinfeld, J. H., Surratt, J. D., Szmigielski, R., and Wildt, J.: The formation, properties and impact of secondary organic aerosol: current and emerging issues, Atmos. Chem. Phys., 9, 5155-5236, doi: 10.5194/acp-9-5155-2009, 2009.

Hamilton, J. F., Lewis, A. C., Reynolds, J. C., Carpenter, L. J., and Lubben, A.: Investigating the composition of organic aerosol resulting from cyclohexene ozonolysis: low molecular weight and heterogeneous reaction products, Atmos. Chem. Phys., 6, 4973-4984, doi: 10.5194/acpd-6-6369-2006, 2006.

Han, J., Shin, B., Lee, M., Hwang, G., Kim, J., Shim, J., Lee, G., and Shim, C.: Variations of surface ozone at Ieodo Ocean Research Station in the East China Sea and the influence of Asian outflows, Atmos. Chem. Phys., 15, 12611-12621, doi: 10.5194/acp-15-12611-2015, 2015.

Heintzenberg, J., Birmili, W., Otto, R., Andreae, M. O., Mayer, J. C., Chi, X., and Panov, A.: Aerosol particle number size distributions and particulate light absorption at the ZOTTO tall tower (Siberia), 2006–2009, Atmos. Chem. Phys., 11, 8703-8719, doi: 10.5194/acp-11-8703-2011, 2011.

Hu, L., Millet, D. B., Mohr, M. J., Wells, K. C., Griffis, T. J., and Helmig, D.: Sources and seasonality of atmospheric methanol based on tall tower measurements in the US Upper Midwest, Atmos. Chem. Phys., 11, 11145-11156, doi: 10.5194/acp-11-11145-2011, 2011.

Ho, K. F., Ho, S. S. H., Lee, S. C., Kawamura, K., Zou, S. C., Cao, J. J., and Xu, H. M.: Summer and winter variations of dicarboxylic acids, fatty acids and benzoic acid in PM2.5 in Pearl Delta River Region, China, Atmos. Chem. Phys., 10, 26677-26703, 2011.

Huang, R.-J., Zhang, Y., Bozzetti, C., Ho, K.-F., Cao, J.-J., Han, Y., Daellenbach, K. R., Slowik, J. G., Platt, S. M., and Canonaco, F.: High secondary aerosol contribution to particulate pollution during haze events in China, Nature, 514, 218-222, 2014.

Jung, J., Tsatsral, B., Kim, Y. J., and Kawamura, K.: Organic and inorganic aerosol compositions in Ulaanbaatar, Mongolia, during the cold winter of 2007 to 2008: Dicarboxylic acids, ketocarboxylic acids, andα-dicarbonyls, J. Geophys. Res., 115,

10.1029/2010jd014339, 2010.

Kanakidou, M., Seinfeld, J., Pandis, S., Barnes, I., Dentener, F., Facchini, M., Dingenen, R. V., Ervens, B., Nenes, A., and Nielsen, C.: Organic aerosol and global climate modelling: a review, Atmos. Chem. Phys., 5, 1053-1123, https://doi.org/10.5194/acp-5-1053-2005, 2005.

Kautzman, K. E., Surratt, J. D., Chan, M. N., Chan, A. W. H., Hersey, S. P., Chhabra, P. S., Dalleska, N. F., Wennberg, P. O., Flagan, R. C., and Seinfeld, J. H.: Chemical composition of gas- and aerosol-phase products from the photooxidation of naphthalene, J. Phys. Chem. A, 114, 913-934, doi: 10.1021/jp908530s, 2010.

Kawamura, K., and Gagosian, R.: Implications of ω-oxocarboxylic acids in the remote marine atmosphere for photo-oxidation of unsaturated fatty acids, Nature, 325, 330-332, 1987.

Kawamura, K., and Kaplan, I. R.: Motor exhaust emissions as a primary source for dicarboxylic acids in Los Angeles ambient air, Environ. Sci. Technol., 21, 105-110, doi: 10.1021/es00155a014, 1987.

Kawamura, K., and Ikushima, K.: Seasonal changes in the distribution of dicarboxylic acids in the urban atmosphere, Environ. Sci. Technol., 27, 2227-2235, doi: 10.1021/es00047a033, 1993.

Kawamura, K., Kasukabe, H., and Barrie, L. A.: Source and reaction pathways of dicarboxylic acids, ketoacids and dicarbonyls in arctic aerosols: one year of observations, Atmos. Environ., 30, 1709-1722, https://doi.org/10.1016/1352-2310(95)00395-9, 1996.

Kawamura, K., and Sakaguchi, F.: Molecular distributions of water soluble dicarboxylic acids in marine aerosols over the Pacific Ocean including tropics, J. Geophys. Res. Atmos., 104, 3501-3509, https://doi.org/10.1029/1998JD100041, 1999.

Kawamura, K., Steinberg, S., Lai, N., and Kaplan, I. R.: Wet deposition of low molecular weight mono- and di-carboxylic acids, aldehydes and inorganic species in Los Angeles, Atmos. Environ., 35, 3917-3926, 2001.

Kawamura, K., Kasukabe, H., and Barrie, L. A.: Secondary formation of water-soluble organic acids and α-dicarbonyls and their contributions to total carbon and water-soluble organic carbon : photochemical aging of organic aerosols in the Arctic spring, J. Geophys. Res. Atmos., 115, https://doi.org/10.1029/2010JD014299, 2010.

Kawamura, K., and Pavuluri, C. M.: New Directions: need for better understanding of plastic waste burning as inferred from high abundance of terephthalic acid in South Asian aerosols, Atmos. Environ., 44, 5320-5321, doi: 10.1016/j.atmosenv.2010.09.016, 2010.

Kawamura, K., Tachibana, E., Okuzawa, K., Aggarwal, S., Kanaya, Y., and Wang, Z.: High abundances of water-soluble dicarboxylic acids, ketocarboxylic acids and α-dicarbonyls in the mountaintop aerosols over the North China Plain during wheat burning season, Atmos. Chem. Phys., 13, 8285-8302, https://doi.org/10.5194/acp-13-8285-2013, 2013.

Kawamura, K., and Bikkina, S.: A review of dicarboxylic acids and related compounds in atmospheric aerosols: molecular distributions, sources and transformation, Atmos. Res., 170, 140-160, 2016.

Laskin, A., Moffet, R. C., Gilles, M. K., Fast, J. D., Zaveri, R. A., Wang, B., Nigge, P., and Shutthanandan, J.: Tropospheric chemistry of internally mixed sea salt and organic particles: surprising reactivity of NaCl with weak organic acids, J. Geophys. Res. Atmos., 117, doi:10.1029/2012JD017743, 2012.

Legrand, M., and Angelis, M. D.: Light carboxylic acids in Greenland ice: a record of past forest fires and vegetation emissions from the boreal zone, J. Geophys. Res. Atmos., 101, 4129-4145, https://doi.org/10.1029/95JD03296, 1996.

Li, Z., Guo, J., Ding, A., Liao, H., Liu, J., Sun, Y., Wang, T., Xue, H., Zhang, H., and Zhu, B.: Aerosol and boundary-layer interactions and impact on air quality, Nat Sci Rev, 4, 810-833, doi: 10.1093/nsr/nwx117, 2017.

Liang, P., Zhu, T., Fang, Y., Li, Y., Han, Y., Wu, Y., Hu, M., and Wang, J.: The role of meteorological conditions and pollution control strategies in reducing air pollution in Beijing during APEC 2014 and Victory Parade 2015, Atmos. Chem. Phys., 17, 13921-13940, doi: 10.5194/acp-17-13921-2017, 2017.

Lim, H.-J., Carlton, A. G., and Turpin, B. J.: Isoprene forms secondary organic aerosol through cloud processing: model simulations, Environ. Sci. Technol., 39, 4441-4446, doi: 10.1021/es048039h, 2005.

Magda, C., Bim, G., Gyorgy, V., Wu, W., Reinhilde, V., Vlada, P., Jan, C., Pascal, G., Andreae, M. O., and Paulo, A.: Formation of secondary organic aerosols through photooxidation of isoprene, Science, 303, 1173-1176, doi: 10.1126/science.1092805, 2004.

Matsunaga, S., Kawamura, K., Nakatsuka, T., and Ohkouchi, N.: Preliminary study on laboratory photochemical formation of low molecular weight dicarboxylic acids from unsaturated fatty acid (oleic acid), Res. Org. Geochem., 14, 19-25, doi: 10.20612/rog.14.0_19, 1999.

Meng, J., Wang, G., Li, J., Cheng, C., Ren, Y., Huang, Y., Cheng, Y., Cao, J., and Zhang, T.: Seasonal characteristics of oxalic acid and related SOA in the free troposphere of Mt. Hua, central China: implications for sources and formation mechanisms, Sci. Tot. Environ., 493, 1088-1097, https://doi.org/10.1016/j.scitotenv.2014.04.086, 2014.

Mikhailov, E. F., Mironova, S., Mironov, G., Vlasenko, S., Panov, A., Chi, X., Walter, D., Carbone, S., Artaxo, P., Heimann, M., Lavric, J., Pöschl, U., and Andreae, M. O.: Long-term measurements (2010–2014) of carbonaceous aerosol and carbon monoxide at the Zotino Tall Tower Observatory (ZOTTO) in central Siberia, Atmos. Chem. Phys., 17, 14365-14392, doi: 10.5194/acp-17-14365-2017, 2017.

Mochida, M., Umemoto, N., Kawamura, K., Lim, H.-J., and Turpin, B. J.: Bimodal size distributions of various organic acids and fatty acids in the marine atmosphere: Influence of anthropogenic aerosols, Asian dusts, and sea spray off the coast of East Asia, J. Geophys. Res., 112, doi: 10.1029/2006jd007773, 2007.

Morton, D. C., Nagol, J., Carabajal, C. C., Rosette, J., Palace, M., Cook, B. D., Vermote, E. F., Harding, D. J., and North, P. R. J.: Amazon forests maintain consistent canopy structure and greenness during the dry season, Nature, 506, 221-224, doi: 10.1038/nature13006, 2014.

Müller, C., Iinuma, Y., Böge, O., and Herrmann, H.: Applications of CE-ESI-MS/MS analysis to structural elucidation of methylenecyclohexane ozonolysis products in the particle phase, Electrophoresis, 28, 1364-1370, doi: 10.1002/elps.200600585, 2007.

Narukawa, M., Kawamura, K., Takeuchi, N., and Nakajima, T.: Distribution of dicarboxylic acids and carbon isotopic compositions in aerosols from 1997 Indonesian forest fires, Geophys. Res. Lett., 26, 3101–3104, https://doi.org/10.1029/1999GL010810, 1999.

Pathak, R. K., Wang, T., Ho, K., and Lee, S.: Characteristics of summertime PM2.5 organic and elemental carbon in four major Chinese cities: implications of high acidity for water-soluble organic carbon (WSOC), Atmos. Environ., 45, 318-325, doi: 10.1016/j.atmosenv.2010.10.021, 2011.

Pavuluri, C. M., and Kawamura, K.: Evidence for 13-carbon enrichment in oxalic acid via iron catalyzed photolysis in aqueous phase, Geophys. Res. Lett., 39, 3802, https://doi.org/10.1029/2011GL050398, 2012.

Pavuluri, C. M., Kawamura, K., Mihalopoulos, N., and Swaminathan, T.: Laboratory photochemical processing of aqueous

aerosols : formation and degradation of dicarboxylic acids, oxocarboxylic acids and alpha-dicarbonyls, Atmospheric Chemistry and Physics, 15, 7999-8012, 2015.

Pöhlker, C., Walter, D., Paulsen, H., Könemann, T., Rodríguez-Caballero, E., Moran-Zuloaga, D., Brito, J., Carbone, S., Degrendele, C., Després, V. R., Ditas, F., Holanda, B. A., Kaiser, J. W., Lammel, G., Lavrič, J. V., Ming, J., Pickersgill, D., Pöhlker, M. L., Praß, M., Löbs, N., Saturno, J., Sörgel, M., Wang, Q., Weber, B., Wolff, S., Artaxo, P., Pöschl, U., and Andreae, M. O.: Land cover and its transformation in the backward trajectory footprint region of the Amazon Tall Tower Observatory, Atmos. Chem. Phys., 19, 8425-8470, 10.5194/acp-19-8425-2019, 2019.

Quesada, C. A., Phillips, O. L., Schwarz, M., Czimczik, C. I., Baker, T. R., Patiño, S., Fyllas, N. M., Hodnett, M. G., Herrera, R., Almeida, S., Alvarez Dávila, E., Arneth, A., Arroyo, L., Chao, K. J., Dezzeo, N., Erwin, T., di Fiore, A., Higuchi, N., Honorio Coronado, E., Jimenez, E. M., Killeen, T., Lezama, A. T., Lloyd, G., López-González, G., Luizão, F. J., Malhi, Y., Monteagudo, A., Neill, D. A., Núñez Vargas, P., Paiva, R., Peacock, J., Peñuela, M. C., Peña Cruz, A., Pitman, N., Priante Filho, N., Prieto, A., Ramírez, H., Rudas, A., Salomão, R., Santos, A. J. B., Schmerler, J., Silva, N., Silveira, M., Vásquez, R., Vieira, I., Terborgh, J., and Lloyd, J.: Basin-wide variations in Amazon forest structure and function are mediated by both soils and climate, Biogeosciences, 9, 2203-2246, doi: 10.5194/bg-9-2203-2012, 2012.

Rinaldi, M., Decesari, S., Carbone, C., Finessi, E., Fuzzi, S., Ceburnis, D., O'Dowd, C. D., Sciare, J., Burrows, J. P., Vrekoussis, M., Ervens, B., Tsigaridis, K., and Facchini, M. C.: Evidence of a natural marine source of oxalic acid and a possible link to glyoxal, J. Geophys. Res. Atmos., 116, 971-978, https://doi.org/10.1029/2011JD015659, 2011.

Rizzo, L. V., Artaxo, P., Müller, T., Wiedensohler, A., Paixão, M., Cirino, G. G., Arana, A., Swietlicki, E., Roldin, P., Fors, E. O., Wiedemann, K. T., Leal, L. S. M., and Kulmala, M.: Long term measurements of aerosol optical properties at a primary forest site in Amazonia, Atmos. Chem. Phys., 13, 2391-2413, doi: 10.5194/acp-13-2391-2013, 2013.

Rogge, W. F., Hildemann, L. M., Mazurek, M. A., Cass, G. R., and Simoneit, B. R.: Sources of fine organic aerosol. 1. Charbroilers and meat cooking operations, Environ. Sci. Technol., 25, 1112-1125, 1991.

Rogge, W. F., Hildemann, L. M., Mazurek, M. A., Cass, G. R., and Simoneit, B. R.: Sources of fine organic aerosol. 2. Noncatalyst and catalyst-equipped automobiles and heavy-duty diesel trucks, Environ. Sci. Technol., 27, 636-651, doi: 10.1021/es00041a007, 1993.

Sandradewi, J., Prévôt, A. S. H., Szidat, S., Perron, N., Alfarra, M. R., Lanz, V. A., Weingartner, E., and Baltensperger, U.: Using aerosol light absorption measurements for the quantitative determination of wood burning and traffic emission contributions to particulate matter, Environ. Sci. Technol., 42, 3316-3323, doi: 10.1021/es702253m, 2008.

Saturno, J., Holanda, B. A., Pöhlker, C., Ditas, F., Wang, Q., Moran-Zuloaga, D., Brito, J., Carbone, S., Cheng, Y., Chi, X., Ditas, J., Hoffmann, T., Hrabe de Angelis, I., Könemann, T., Lavrič, J. V., Ma, N., Ming, J., Paulsen, H., Pöhlker, M. L., Rizzo, L. V., Schlag, P., Su, H., Walter, D., Wolff, S., Zhang, Y., Artaxo, P., Pöschl, U., and Andreae, M. O.: Black and brown carbon over central Amazonia: long-term aerosol measurements at the ATTO site, Atmos. Chem. Phys., 18, 12817-12843, doi: 10.5194/acp-18-12817-2018, 2018.

Sempére, R., and Kawamura, K.: Comparative distributions of dicarboxylic acids and related polar compounds in snow, rain and aerosols from urban atmosphere, Atmos. Environ., 28, 449-459, https://doi.org/10.1016/1352-2310(94)90123-6, 1994.

Sharkey, T. D., Wiberley, A. E., and Donohue, A. R.: Isoprene emission from plants: why and how, Annals of Botany, 101, 5-18, doi: 10.1093/aob/mcm240, 2007.

Simoneit, B. R., Medeiros, P. M., and Didyk, B. M.: Combustion products of plastics as indicators for refuse burning in the atmosphere, Environ. Sci. Technol., 39, 6961-6970, doi: 10.1021/es050767x, 2005.

Simoneit, B. R. T.: Biomass burning - a review of organic tracers for smoke from incomplete combustion, Appl. Geochem., 17, 129-162, https://doi.org/10.1016/S0883-2927(01)00061-0, 2002.

Stephanou, E. G., and Stratigakis, N.: Oxocarboxylic and. alpha, omega-dicarboxylic acids: photooxidation products of biogenic unsaturated fatty acids present in urban aerosols, Environ. Sci. Technol., 27, 1403-1407, doi: 10.1021/es00044a016, 1993.

Strader, R., Lurmann, F., and Pandis, S. N.: Evaluation of secondary organic aerosol formation in winter, Atmos. Environ., 33, 4849-4863, https://doi.org/10.1016/S1352-2310(99)00310-6, 1999.

Sun, J., Mahrt, L., Banta, R. M., and Pichugina, Y. L.: Turbulence Regimes and Turbulence Intermittency in the Stable Boundary Layer during CASES-99, J. Atmos. Sci., 69, 338-351, doi: 10.1175/JAS-D-11-082.1, 2011.

Sun, Y., Wang, Z., Dong, H., Yang, T., Li, J., Pan, X., Chen, P., and Jayne, J. T.: Characterization of summer organic and inorganic aerosols in Beijing, China with an aerosol chemical speciation monitor, Atmos. Environ., 51, 250-259, doi: 10.1016/j.atmosenv.2012.01.013, 2012.

Sun, Y., Jiang, Q., Xu, Y., Ma, Y., Zhang, Y., Liu, X., Li, W., Wang, F., Li, J., Wang, P., and Li, Z.: Aerosol characterization over the North China Plain: Haze life cycle and biomass burning impacts in summer, J. Geophys. Res. Atmos., 121, 2508-2521, doi: 10.1002/2015jd024261, 2016.

Surratt, J. D., Chan, A. W. H., Eddingsaas, N. C., Chan, M., Loza, C. L., Kwan, A. J., Hersey, S. P., Flagan, R. C., Wennberg, P. O., and Seinfeld, J. H.: Reactive intermediates revealed in secondary organic aerosol formation from isoprene, Proc. Nat. Acad. Sci. U.S.A., 107, 6640, doi: 10.1073/pnas.0911114107, 2010.

Tan, Y., Carlton, A. G., Seitzinger, S. P., and Turpin, B. J.: SOA from methylglyoxal in clouds and wet aerosols: Measurement and prediction of key products, Atmos. Environ., 44, 5218-5226, https://doi.org/10.1016/j.atmosenv.2010.08.045, 2010.

Tedetti, M., Kawamura, K., Charrière, B., Chevalier, N., and Sempéré, R.: Determination of low molecular weight dicarboxylic and ketocarboxylic acids in seawater samples, Anal. Chem., 78, 6012-6018, doi: 10.1021/ac052226w, 2006.

Trebs, I., Mayol-Bracero, O. L., Pauliquevis, T., Kuhn, U., Sander, R., Ganzeveld, L., Meixner, F. X., Kesselmeier, J., Artaxo, P., and Andreae, M. O.: Impact of the Manaus urban plume on trace gas mixing ratios near the surface in the Amazon Basin: Implications for the NO-NO2-O3 photostationary state and peroxy radical levels, J. Geophys. Res. Atmos., 117, doi: 10.1029/2011JD016386, 2012.

Turpin, B. J., and Huntzicker, J. J.: Secondary formation of organic aerosol in the Los Angeles basin: a descriptive analysis of organic and elemental carbon concentrations, Atmospheric Environment. Part A. General Topics, 25, 207-215, https://doi.org/10.1016/0960-1686(91)90291-E, 1991.

Turpin, B. J., and Huntzicker, J. J.: Identification of secondary organic aerosol episodes and quantitation of primary and secondary organic aerosol concentrations during SCAQS, Atmos. Environ., 29, 3527-3544, https://doi.org/10.1016/1352-2310(94)00276-Q, 1995.

Volkamer, R., Platt, U., and Wirtz, K.: Primary and secondary glyoxal formation from aromatics: experimental evidence for the bicycloalkyl-radical pathway from benzene, toluene, and p-xylene, J. Phys. Chem. A, 105, 7865-7874, doi: 10.1021/jp010152w, 2001.

Wang, G., Kawamura, K., Lee, S., Ho, K., and Cao, J.: Molecular, Seasonal, and Spatial Distributions of Organic Aerosols from Fourteen Chinese Cities, Environ. Sci. Technol., 40, 4619-4625, doi: 10.1021/es060291x, 2006a.

Wang, G., Kawamura, K., Watanabe, T., Lee, S., Ho, K., and Cao, J.: High loadings and source strengths of organic aerosols in China, Geophys. Res. Lett., 33, doi: 10.1029/2006gl027624, 2006b.

Wang, G., Kawamura, K., Cheng, C., Li, J., Cao, J., Zhang, R., Zhang, T., Liu, S., and Zhao, Z.: Molecular distribution and stable carbon isotopic composition of dicarboxylic acids, ketocarboxylic acids, and α-dicarbonyls in size-resolved atmospheric particles from Xi'an City, China, Environ. Sci. Technol., 46, 4783-4791, doi: 10.1021/es204322c, 2012.

Wang, G., Zhang, R., Gomez, M. E., Yang, L., Levy, Z. M., Hu, M., Lin, Y., Peng, J., Guo, S., and Meng, J.: Persistent sulfate formation from London Fog to Chinese haze, Proc Natl Acad Sci U S A, 48, 13630-13635, 2016.

Wang, H., Kawamura, K., and Yamazaki, K.: Water-soluble dicarboxylic acids, ketoacids and dicarbonyls in the atmospheric aerosols over the Southern Ocean and western Pacific Ocean, J. Atmos. Chem., 53, 43-61, doi: 10.1007/s10874-006-1479-4, 2006c.

Wang, Q., Sun, Y., Xu, W., Du, W., Zhou, L., Tang, G., Chen, C., Cheng, X., Zhao, X., Ji, D., Han, T., Wang, Z., Li, J., and Wang, Z.: Vertically resolved characteristics of air pollution during two severe winter haze episodes in urban Beijing, China, Atmos. Chem. Phys., 18, 2495-2509, doi: 10.5194/acp-18-2495-2018, 2018.

Warneck, P.: In-cloud chemistry opens pathway to the formation of oxalic acid in the marine atmosphere, Atmos. Environ., 37, 2423-2427, doi: 10.1016/S1352-2310(03)00136-5, 2003.

Watson, J. G., Chow, J. C., and Houck, J. E.: PM2.5 chemical source profiles for vehicle exhaust, vegetative burning, geological material, and coal burning in Northwestern Colorado during 1995, Chemosphere, 43, 1141-1151, doi: 10.1016/S0045-6535(00)00171-5, 2001.

Winderlich, J., Chen, H., Gerbig, C., Seifert, T., Kolle, O., Lavrič, J. V., Kaiser, C., Höfer, A., and Heimann, M.: Continuous low-maintenance CO2/CH4/H2O measurements at the Zotino Tall Tower Observatory (ZOTTO) in Central Siberia, Atmos. Meas. Tech., 3, 1113-1128, doi: 10.5194/amt-3-1113-2010, 2010.

Xia, X., Chen, H., and Zhang, W.: Analysis of the dependence of column-integrated aerosol properties on long-range transport of air masses in Beijing, Atmos. Environ., 41, 7739-7750, doi: 10.1016/j.atmosenv.2007.06.042, 2007.

Xie, Q. R., Li, Y., Yue, S. Y., Su, S. H., Cao, D., Xu, Y. S., Chen, J., Tong, H. J., Su, H., Cheng, Y. F., Zhao, W. Y., Hu, W., Wang, Z., Yang, T., Pan, X. L., Sun, Y. L., Wang, Z. F., Liu, C. Q., Kawamura, K., Jiang, G. B., Shiraiwa, M., and Fu, P. Q.: Increase of High Molecular Weight Organosulfate With Intensifying Urban Air Pollution in the Megacity Beijing, Journal of Geophysical Research-Atmospheres, 125, e2019JD032200, 10.1029/2019jd032200, 2020.

Xu, W., Song, W., Zhang, Y., Liu, X., Zhang, L., Zhao, Y., Liu, D., Tang, A., Yang, D., Wang, D., Wen, Z., Pan, Y., Fowler, D., Collett Jr, J. L., Erisman, J. W., Goulding, K., Li, Y., and Zhang, F.: Air quality improvement in a megacity: implications from 2015 Beijing Parade Blue pollution control actions, Atmos. Chem. Phys., 17, 31-46, doi: 10.5194/acp-17-31-2017, 2017.

Yáñez-Serrano, A. M., Nölscher, A. C., Williams, J., Wolff, S., Alves, E., Martins, G. A., Bourtsoukidis, E., Brito, J., Jardine, K., Artaxo, P., and Kesselmeier, J.: Diel and seasonal changes of biogenic volatile organic compounds within and above an Amazonian rainforest, Atmos. Chem. Phys., 15, 3359-3378, doi: 10.5194/acp-15-3359-2015, 2015.

Yáñez-Serrano, A. M., Nölscher, A. C., Bourtsoukidis, E., Gomes Alves, E., Ganzeveld, L., Bonn, B., Wolff, S., Sa, M., Yamasoe, M., Williams, J., Andreae, M. O., and Kesselmeier, J.: Monoterpene chemical speciation in a tropical rainforest:variation with season, height, and time of dayat the Amazon Tall Tower Observatory (ATTO), Atmos. Chem. Phys., 18, 3403-3418, doi: 10.5194/acp-18-3403-2018, 2018.

Yang, J., Zhao, W. Y., Wei, L. F., Zhang, Q., Zhao, Y., Hu, W., Wu, L. B., Li, X. D., Pavuluri, C. M., Pan, X. L., Sun, Y. L., Wang, Z. F., Liu, C. Q., Kawamura, K., and Fu, P. Q.: Molecular and spatial distributions of dicarboxylic acids, oxocarboxylic acids, and alpha-dicarbonyls in marine aerosols from the South China Sea to the eastern Indian Ocean, Atmos. Chem. Phys., 20, 6641-6660, 10.5194/acp-20-6841-2020, 2020.

Yu, X. Y., Cary, R. A., and Laulainen, N. S.: Primary and secondary organic carbon downwind of Mexico City, Atmos. Chem. Phys., 9, 6793-6814, doi: 10.5194/acp-9-6793-2009, 2009.

Yue, S. Y., Ren, H., Fan, S. Y., Wei, L. F., Zhao, J., Bao, M. Y., Hou, S. J., Zhan, J. Q., Zhao, W. Y., Ren, L. J., Kang, M. J., Li, L. J., Zhang, Y. L., Sun, Y. L., Wang, Z. F., and Fu, P. Q.: High Abundance of Fluorescent Biological Aerosol Particles in Winter in Beijing, China, ACS Earth and Space Chemistry, 1, 493-502, 10.1021/acsearthspacechem.7b00062, 2017.

Zhang, Y. L., Ren, H., Sun, Y., Cao, F., Chang, Y., Liu, S., Lee, X., Agrios, K., Kawamura, K., Liu, D., Ren, L., Du, W., Wang, Z., Prévôt, A. S. H., Szidat, S., and Fu, P. Q.: High contribution of nonfossil sources to submicrometer organic aerosols in Beijing, China, Environ. Sci. Technol., 51, 7842-7852, doi: 10.1021/acs.est.7b01517, 2017.

Zhao, J., Du, W., Zhang, Y., Wang, Q., Chen, C., Xu, W., Han, T., Wang, Y., Fu, P., Wang, Z., Li, Z., and Sun, Y.: Insights into aerosol chemistry during the 2015 China Victory Day parade: results from simultaneous measurements at ground level and 260 m in Beijing, Atmos. Chem. Phys., 17, 3215-3232, doi: 10.5194/acp-17-3215-2017, 2017.

Zhao, W. Y., Kawamura, K., Yue, S. Y., Wei, L. F., Ren, H., Yan, Y., Kang, M. J., Li, L. J., Ren, L. J., Lai, S. C., Li, J., Sun, Y. L., Wang, Z. F., and Fu, P. Q.: Molecular distribution and compound-specific stable carbon isotopic composition of dicarboxylic acids, oxocarboxylic acids and alpha-dicarbonyls in $PM_{2.5}$ from Beijing, China, Atmos. Chem. Phys., 18, 2749-2767, 10.5194/acp-18-2749-2018, 2018.

Zhao, W. Y., Fu, P. Q., Yue, S. Y., Li, L. J., Xie, Q. R., Zhu, C., Wei, L. F., Ren, H., Li, P., Li, W. J., Sun, Y. L., Wang, Z. F., Kawamura, K., and Chen, J. M.: Excitation-emission matrix fluorescence, molecular characterization and compound-specific stable carbon isotopic composition of dissolved organic matter in cloud water over Mt. Tai, Atmospheric Environment, 213, 608-619, 10.1016/j.atmosenv.2019.06.034, 2019a.

Zhao, W. Y., Wang, Z., Li, S. W., Li, L. J., Wei, L. F., Xie, Q. R., Yue, S. Y., Li, T., Liang, Y. H., Sun, Y. L., Wang, Z. F., Li, X. D., Kawamura, K., Wang, T., and Fu, P. Q.: Water-soluble low molecular weight organics in cloud water at Mt. Tai Mo Shan, Hong Kong, Science of the Total Environment, 697, 10.1016/j.scitotenv.2019.134095, 2019b.

Zhao, X. J., Zhao, P. S., Xu, J., Meng, W., Pu, W. W., Dong, F., He, D., and Shi, Q. F.: Analysis of a winter regional haze event and its formation mechanism in the North China Plain, Atmos. Chem. Phys., 13, 5685-5696, doi: 10.5194/acp-13-5685-2013, 2013.

Zhu, Y., Huang, L., Li, J., Ying, Q., Zhang, H., Liu, X., Liao, H., Li, N., Liu, Z., Mao, Y., Fang, H., and Hu, J.: Sources of particulate matter in China: Insights from source apportionment studies published in 1987–2017, Environment International, 115, 343-357, https://doi.org/10.1016/j.envint.2018.03.037, 2018.

Zimmermann, J., and Poppe, D.: A supplement for the RADM2 chemical mechanism: the photooxidation of isoprene, Atmos. Environ., 30, 1255-1269, doi: 10.1016/1352-2310(95)00417-3, 1996.

Table 1. Vertical concentrations (μg m^{-3}) of OC, EC, SOC, POC and TC in $PM_{2.5}$ aerosols collected at Beijing.

Species (Abbr.)	The ground level (n = 27)		120 m (n = 25)		260 m (n = 25)	
	Range	Mean/SD	Range	Mean/SD	Range	Mean/SD
OC	3.1–15	6.6/2.5	2.8–18	8.2/4.4	2.5–16	7.7/3.5
EC	0.6–2.6	0.9/0.5	0.4–3.2	1.3/0.7	0.3–3.3	1.3/0.8
SOC	0.0–5.0	2.0/1.1	0.0–12	5.1/2.9	0.0–10	4.7/2.2
POC	2.8–13	4.7/2.3	1.1–8.2	3.2/1.9	0.77–8.2	3.2/2.0
TC	3.6–17	7.6/3.0	3.6–20	9.4/5.1	2.9–21	9.0/4.1

Table 2. Vertical concentrations (ng m^{-3}) of dicarboxylic acids, oxoacids and α-dicarbonyls collected in Beijing from August 15th to September 10th, 2015.

Species (Abbr.)	The ground level (n = 27)		120 m (n = 25)		260 m (n = 25)	
	Range	Mean/SD	Range	Mean/SD	Range	Mean/SD
Dicarboxylic acids						
Oxalic, C_2	46–432	160/90	52–570	210/154	60–650	220/140
Malonic, C_3	7.1–49	22/10	8.6–82	32/25	11–75	34/17
Succinic, C_4	7.3–46	21/10	8.7–87	30/21	9.2–76	31/18
Glutaric, C_5	3.2–17	6.5/3.2	2.8–29	9.2/6.4	3.2–25	9.5/5.2
Adipic, C_6	2.5–14	5.3/2.5	3.7–21	8.2/4.2	4.8–21	13/5.0
Pimeric, C_7	0.7–4.7	1.6/1.1	0.2–7.5	2.5/2.1	0.4–9.4	2.5/2.0
Suberic, C_8	BDL–0.3	BDL/0.1	BDL–0.8	0.1/0.2	BDL–1.2	0.2/0.4
Azelaic, C_9	12–34	18/4.8	4.9–53	21/10	5.6–38	17/7.6
Decanedioic, C_{10}	0.4–3.1	1.3/0.7	0.2–4.2	1.6/1.0	BDL–3.7	1.5/0.8
Undecanedioic, C_{11}	BDL–2.9	1.2/0.6	0.4–6.7	1.5/1.4	0.4–5.3	1.4/1.0
Dodecanedioc, C_{12}	BDL–0.2	BDL	BDL–0.7	0.1/0.2	BDL–0.7	0.2/0.2
Methylmalonic, iC_4	0.4–2.8	0.9/0.5	0.2–4.1	1.2/0.8	0.5–2.3	1.1/0.5
Methylsuccinic, iC_5	0.5–3.8	1.6/0.8	0.6–7.9	2.2/1.8	0.7–6.3	2.2/1.4
2-methylglutaric, iC_6	BDL–1.7	0.5/0.4	0.3–4.8	1.0/0.9	0.3–3.9	1.0/0.8
Maleic, M	0.7–2.6	1.3/0.5	0.5–6.0	1.8/1.2	0.9–4.3	2.0/0.9
Fumaric, F	0.2–3.0	1.4/0.7	0.2–6.3	1.5/1.5	0.5–5.8	1.6/1.3
Methylmaleic, mM	0.7–3.0	1.3/0.5	0.5–7.4	1.9/1.6	0.6–4.2	1.9/1.0
Phthalic, Ph	8.3–61	26/11	8.6–51	23/11	8.2–40	21/7.9
Isophthalic, iPh	0.3–1.3	0.6/0.3	0.2–3.0	1.2/1.0	BDL–8.4	1.0/1.7
Terephthalic, tPh	1.8–49	12/10	3.4–64	15/15	2.8–49	13/11
Malic, hC_4	BDL−1.7	0.3/0.3	0.2–2.4	0.6/0.5	0.1–2.4	0.7/0.5
Oxomalonic, kC_3	0.5–9.6	2.7/2.2	0.6–13	4.0/3.4	0.6–12	4.1/2.5
4-oxopimelic, kC_7	0.5–9.7	3.0/2.2	0.4–13	4.4/3.6	1.1–12	5.0/2.6
Total diacids	99–733	285/143	110–945	370/255	126–1001	380/216
Oxocarboxylic acids						
Pyruvic, Pyr	0.6–17	5.6/3.8	0.8–30	10/9.1	0.7–30	8.5/6.8
Glyoxylic, ωC_2	0.5–44	15/11	2.6–80	21/19	2.5–65	20/17
3-oxopropanoic, ωC_3	0.9–8.2	2.9/1.8	1.3–11	4.1/3.1	1.0–12	3.7/2.4
4-oxobutanoic, ωC_4	1.0–11	4.5/2.5	2.7–21	7.3/4.4	1.9–17	6.9/3.8
5-oxopentanoic, ωC_5	0.3–3.4	1.5/0.7	0.6–4.7	2.0/1.1	0.7–3.9	1.9/0.9
7-oxoheptanoic, ωC_7	1.1–5.4	3.2/1.2	1.3–8.6	4.2/2.2	1.8–8.0	4.0/1.5
8-oxooctanoic, ωC_8	0.7–8.7	4.0/1.9	0.8–15	5.0/3.3	0.1–15	5.0/3.4
9-oxononanoic, ωC_9	0.2–2.4	1.2/0.6	0.3–4.9	1.2/1.0	BDL–4.8	1.4/1.2
Total oxoacids	7.3–95	38/22	1.8–170	56/41	11–150	52/34
α-dicarbonyls						
Glyoxal, Gly	0.5–6.1	2.2/1.2	1.0–13	3.3/2.7	0.8–9.8	3.4/2.3
Methylglyoxal, MeGly	1.4–12	4.1/2.6	1.0–20	5.2/4.0	1.3–22	6.7/5.2
Total dicarbonyls	1.8–17	6.3/3.7	2.2–33	8.5/6.6	2.0–31	10/7.4

BDL: below detection limit, which is ca. 0.005 ng m^{-3} for the target compounds.

Table 3. Abundance and naming of measured ions (μg m^{-3}) and organic tracers (ng m^{-3}) used in the PMF analysis.

Tracers	Grouping	Sources	Mean/SD		
			The ground level	120 m	260 m
PAHs276	indeno[1,2,3-cd]pyrene, benzo[ghi]perylene	Combustion sources (mainly coal combustion)	0.41/0.23	0.24/0.18	0.08/0.06
Levoglucosan		Biomass burning	19/16	21/14	23/15
Hopanes	*αβ*-hopane, *αβS&R*-homohopane, *αβS&R*-bishomohopane	Fossil fuel combustion (e.g. vehicle exhaust, coal combustion)	1.5/0.5	2.0/1.0	1.0/0.6
Isoprene SOA tracers	2-methylglyceric acid, 2-methylthreitol, 2-methylerythritol, C_5-alkene triols	Isoprene derived SOA, plants emissions	31/20	41/38	48/37
SO_4^{2-}		Secondary sulfate formation	36/34	43/46	51/46
NO_3^-		Secondary nitrate formation	20/19	29/30	36/43

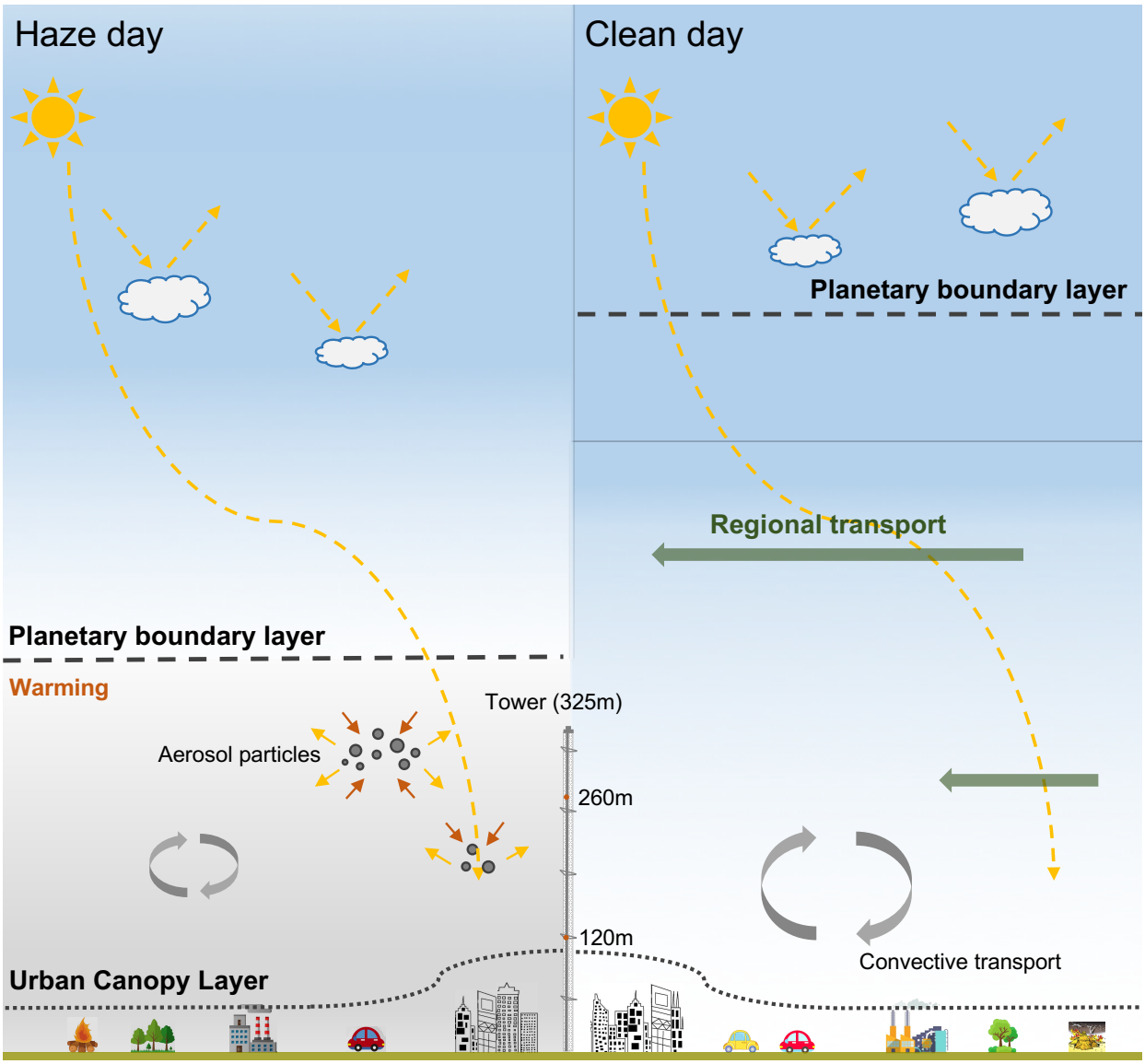

Figure 1. A schematic cartoon showing the atmospheric vertical structure over Beijing in polluted and clean days.

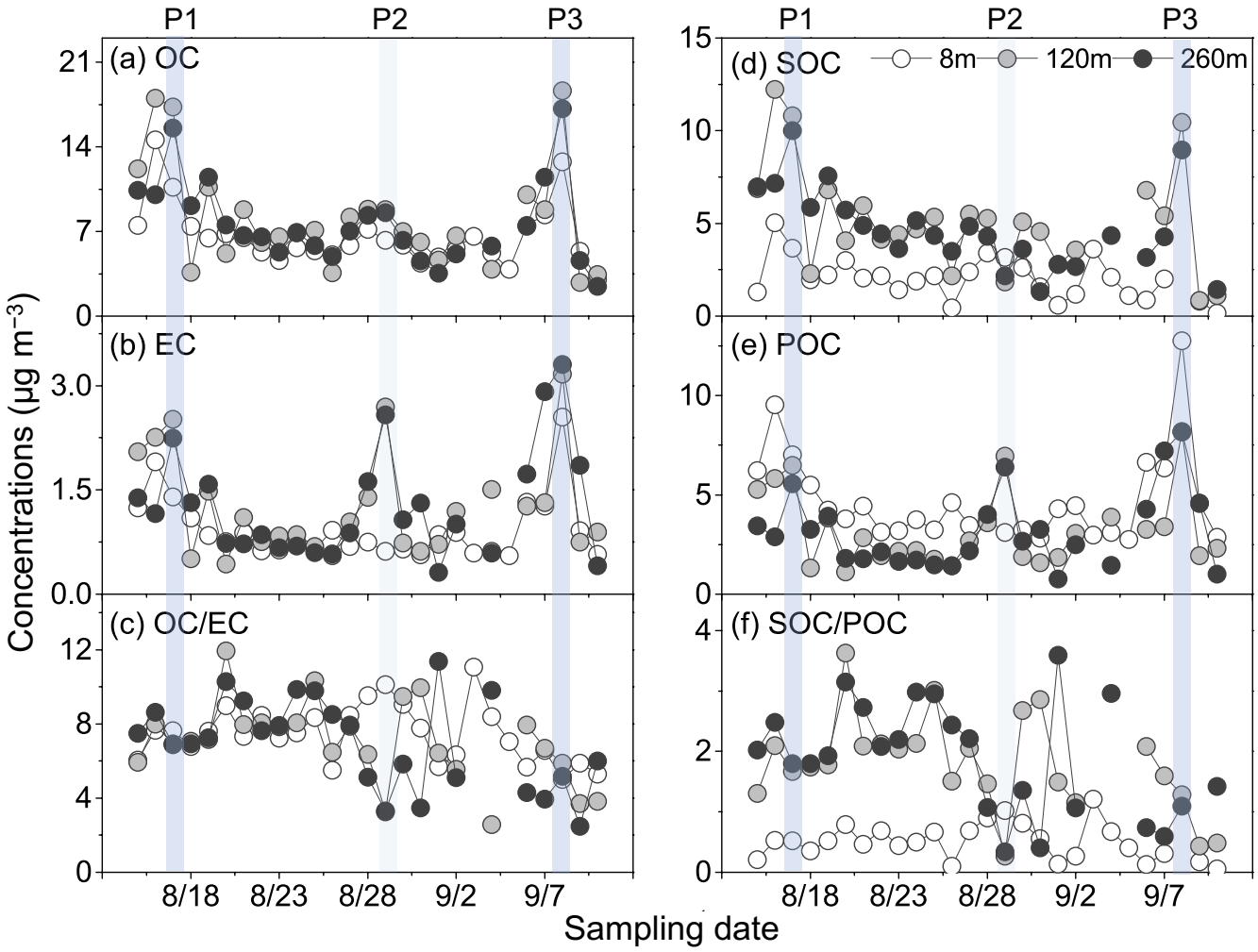

Figure 2. Daily variations in the concentrations of (a) OC, (b) EC, (c) OC/EC, (d) SOC, (e) POC and (f) SOC/POC at three sampling heights in Beijing. Two moderately polluted days (P1 and P3) and one lightly polluted day (P2) are marked for further discussions.

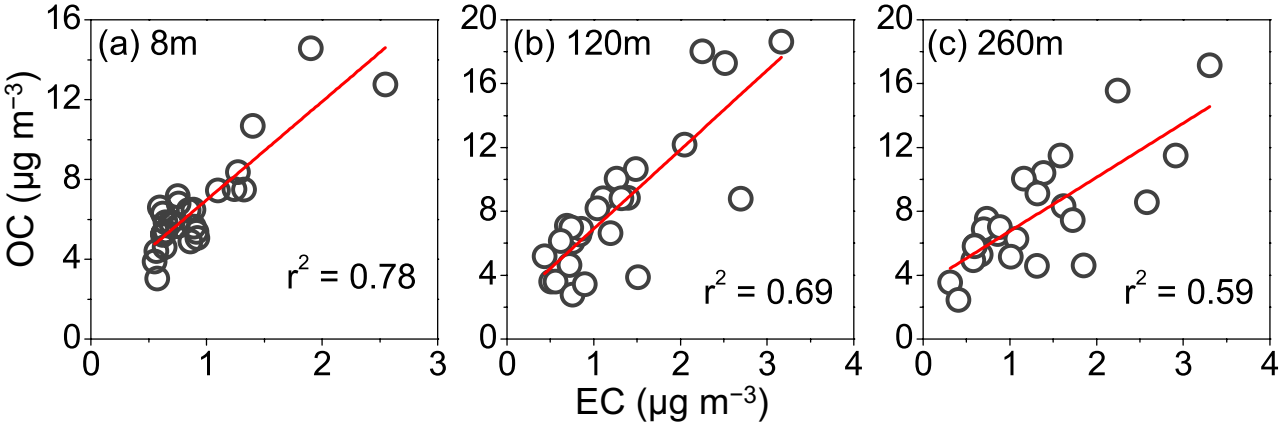

Figure 3. Correlations between OC and EC at the ground level, 120 m and 260 m.

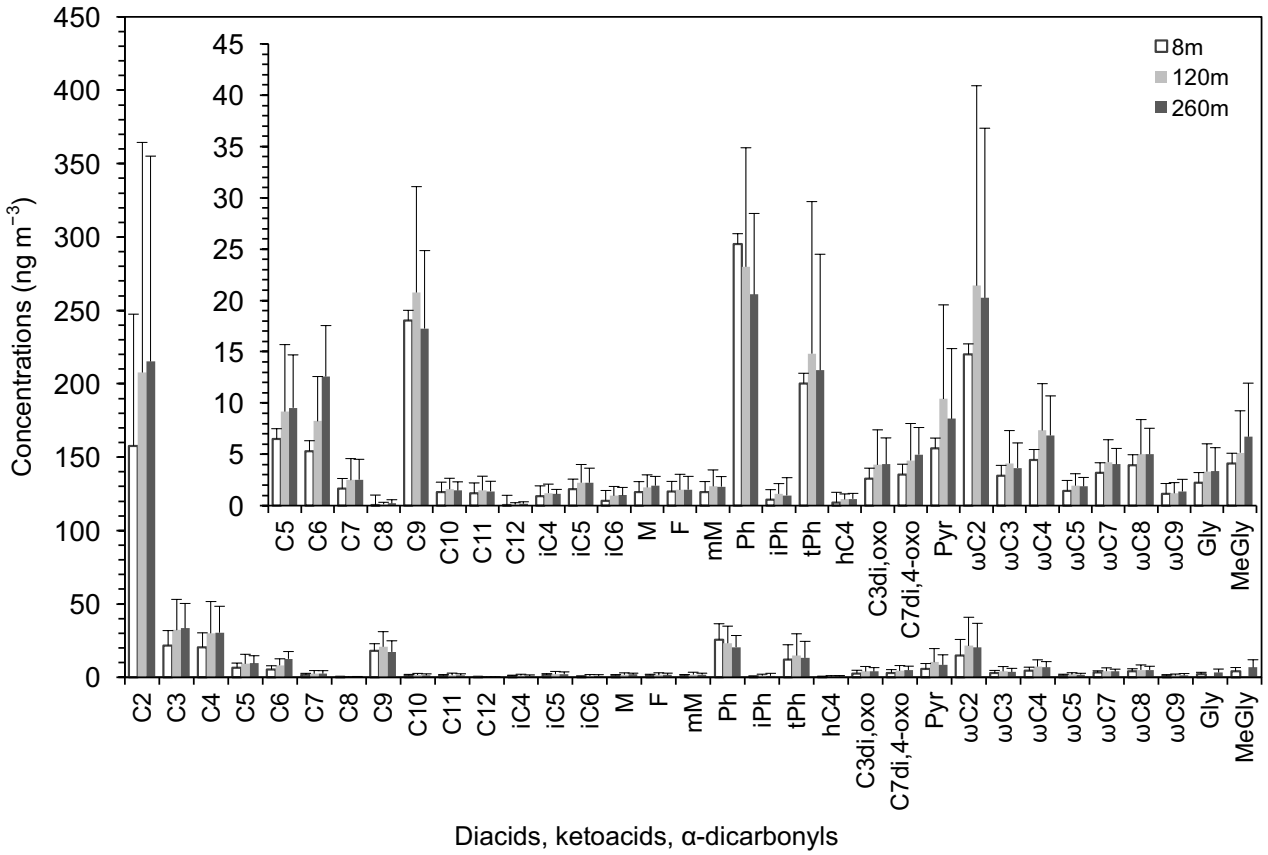

Figure 4. Molecular distributions of dicarboxylic acids and related compounds in the $PM_{2.5}$ samples collected at the tower from 15th August to 10th September 2015 in Beijing.

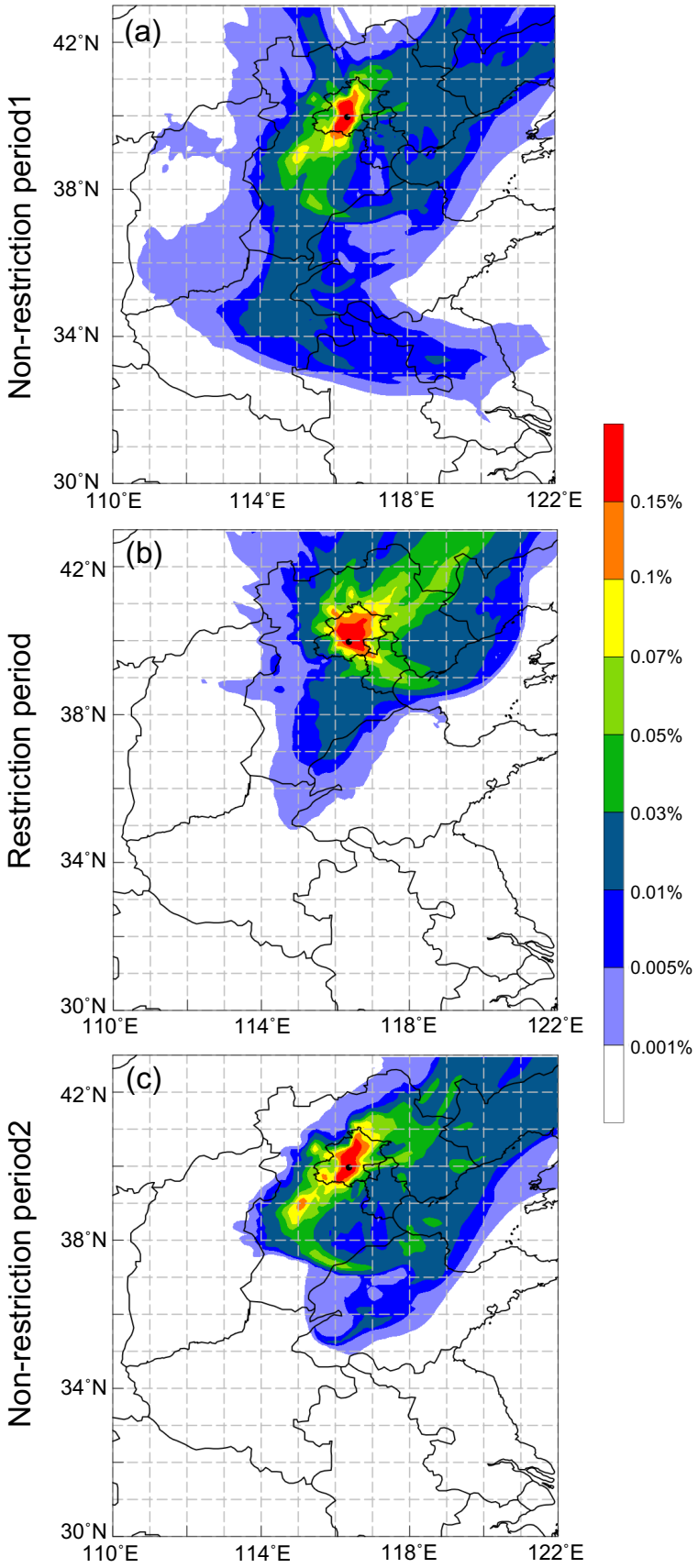

Figure 5. Aerosols footprint regions of non-restriction and restriction periods. The color bar indicates the relative residence time of tracer particles. And the black dot represents the sampling site.

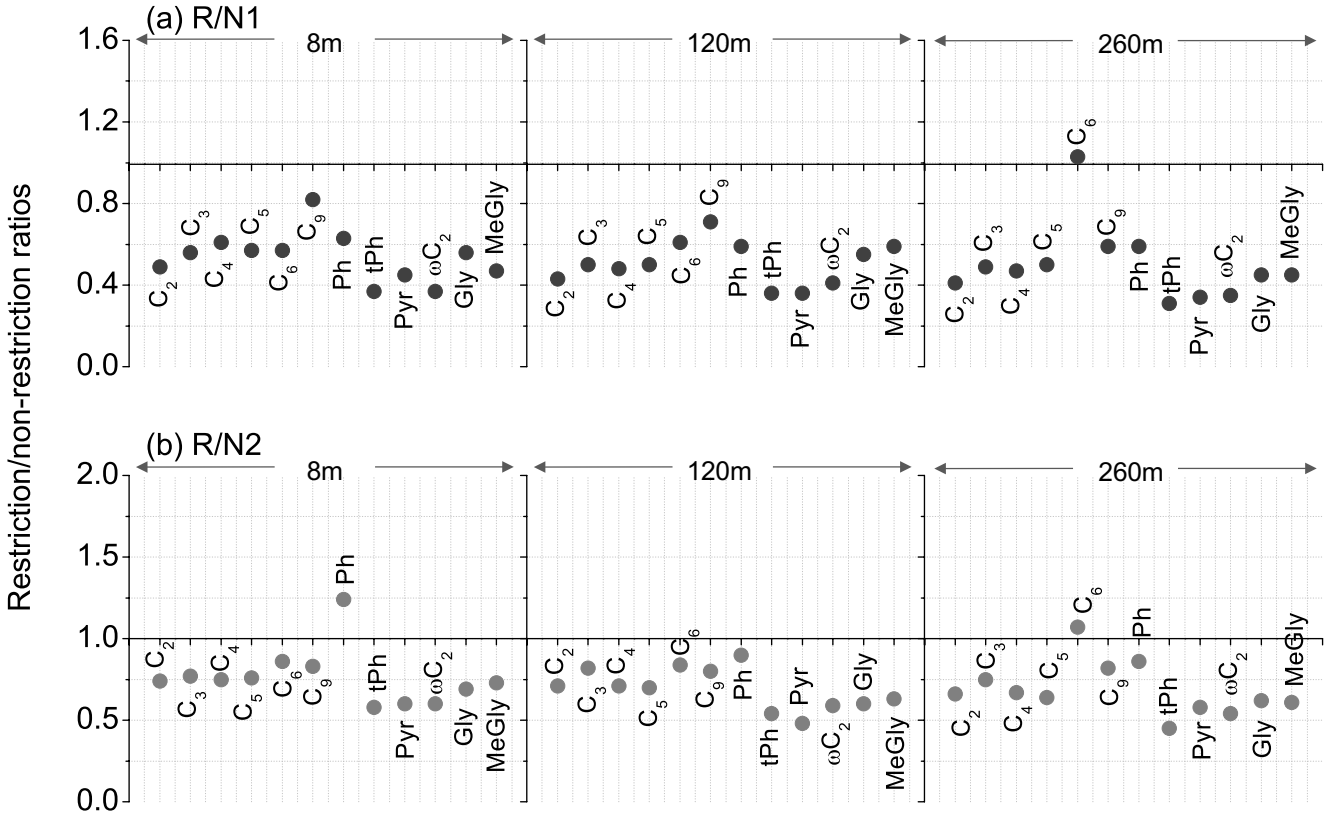

Figure 6. The R/N ratios of diacids and related compounds observed at the tower in Beijing in summer 2015.

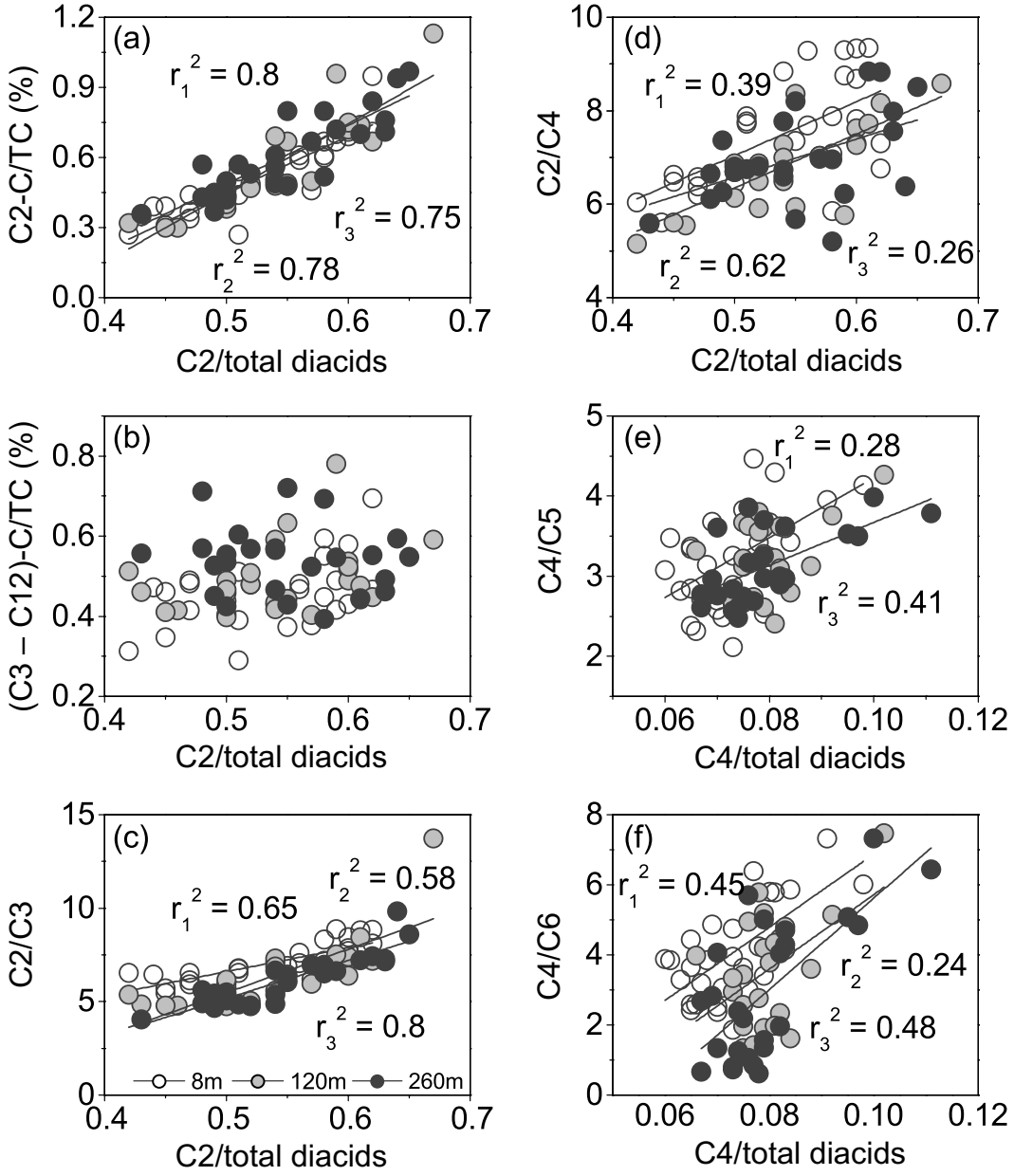

Figure 7. Contributions of (a) C_2-C/TC (%), (b) (C_3–C_{12})-C/TC (%), (c) C_2/C_3 and (d) C_2/C_4 ratios as a function of relative abundance of C_2 in total diacids, as well as correlations for C_4/total diacids with (e) C_4/C_5 and (f) C_4/C_6. The r_1^2, r_2^2, and r_3^2 values are the correlation coefficients for those samples collected at 8 m, 120 m and 260 m, respectively.

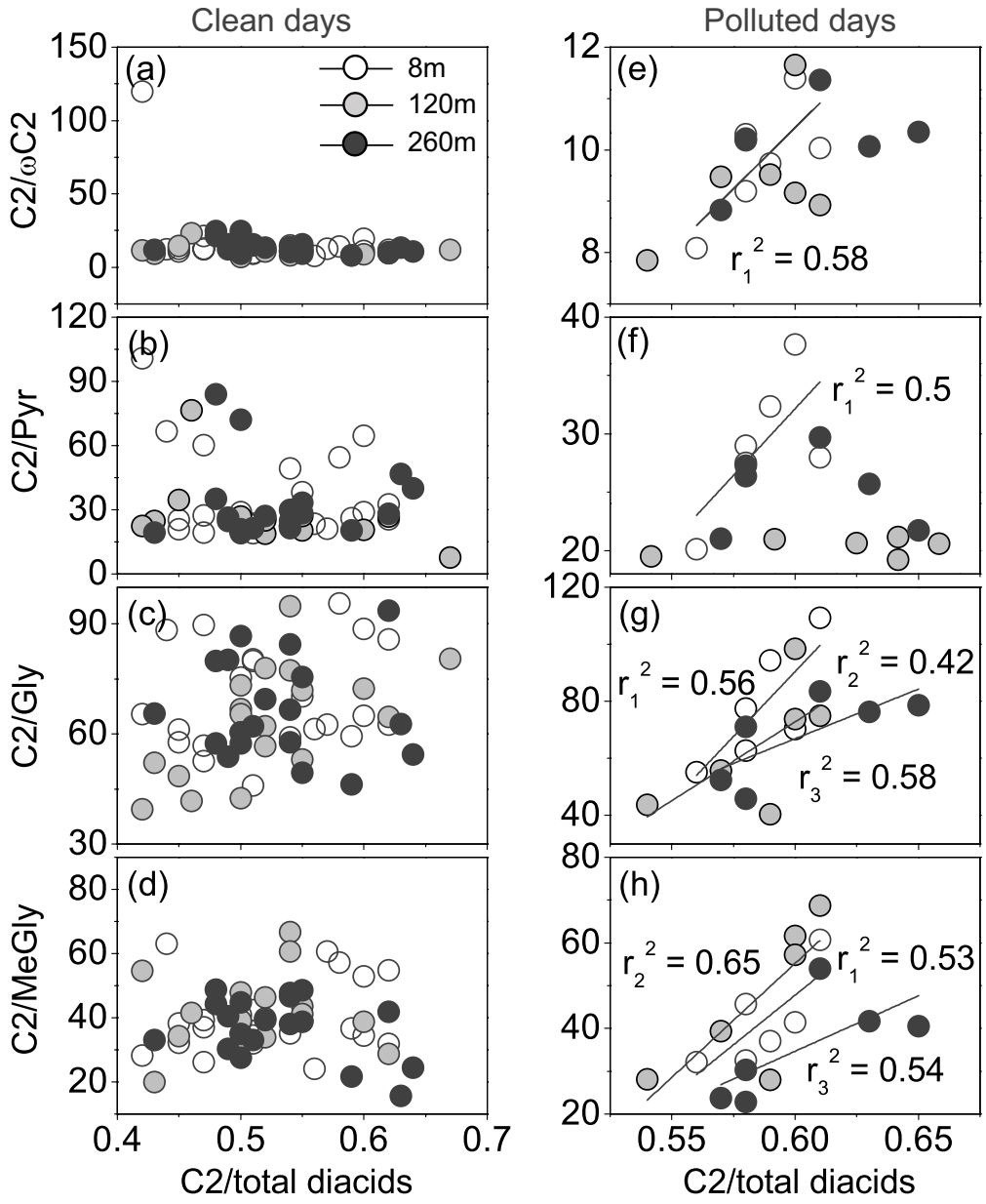

Figure 8. Correlations between concentration ratios of $C_2/\omega C_2$, C_2/Pyr, C_2/Gly, C_2/MeGly and C_2/total diacids in clean days and polluted episodes. The r_1^2, r_2^2, and r_3^2 values represent the correlation coefficients at 8 m, 120 m and 260 m, respectively.

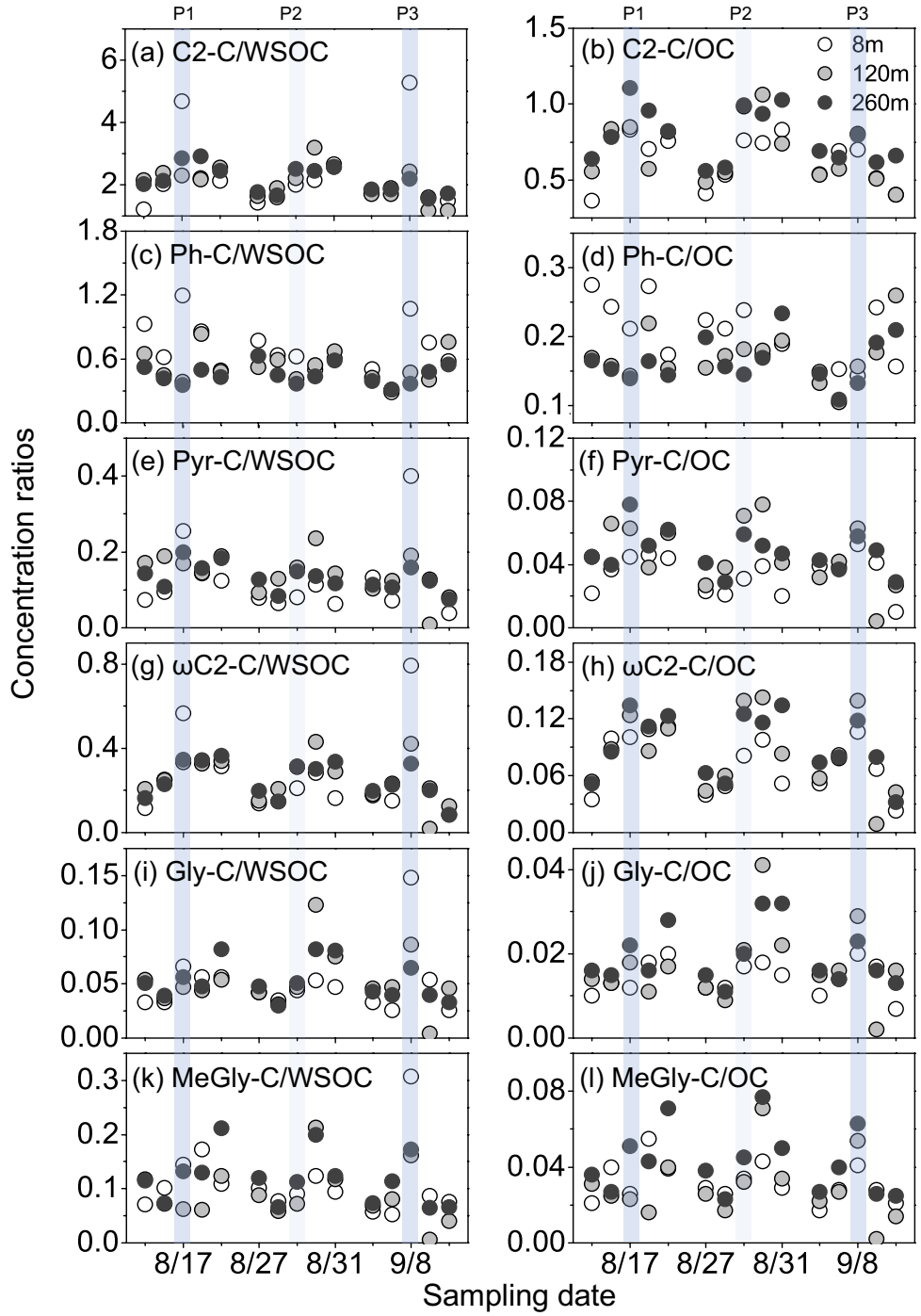

Figure 9. The relative contributions of C_2, Ph, ωC_2, Pyr, Gly and MeGly to carbonaceous fractions (WSOC and OC) in clean, transformation and polluted days. Two moderately polluted days (P1 and P3) and one lightly polluted day (P2) are marked for further discussions.

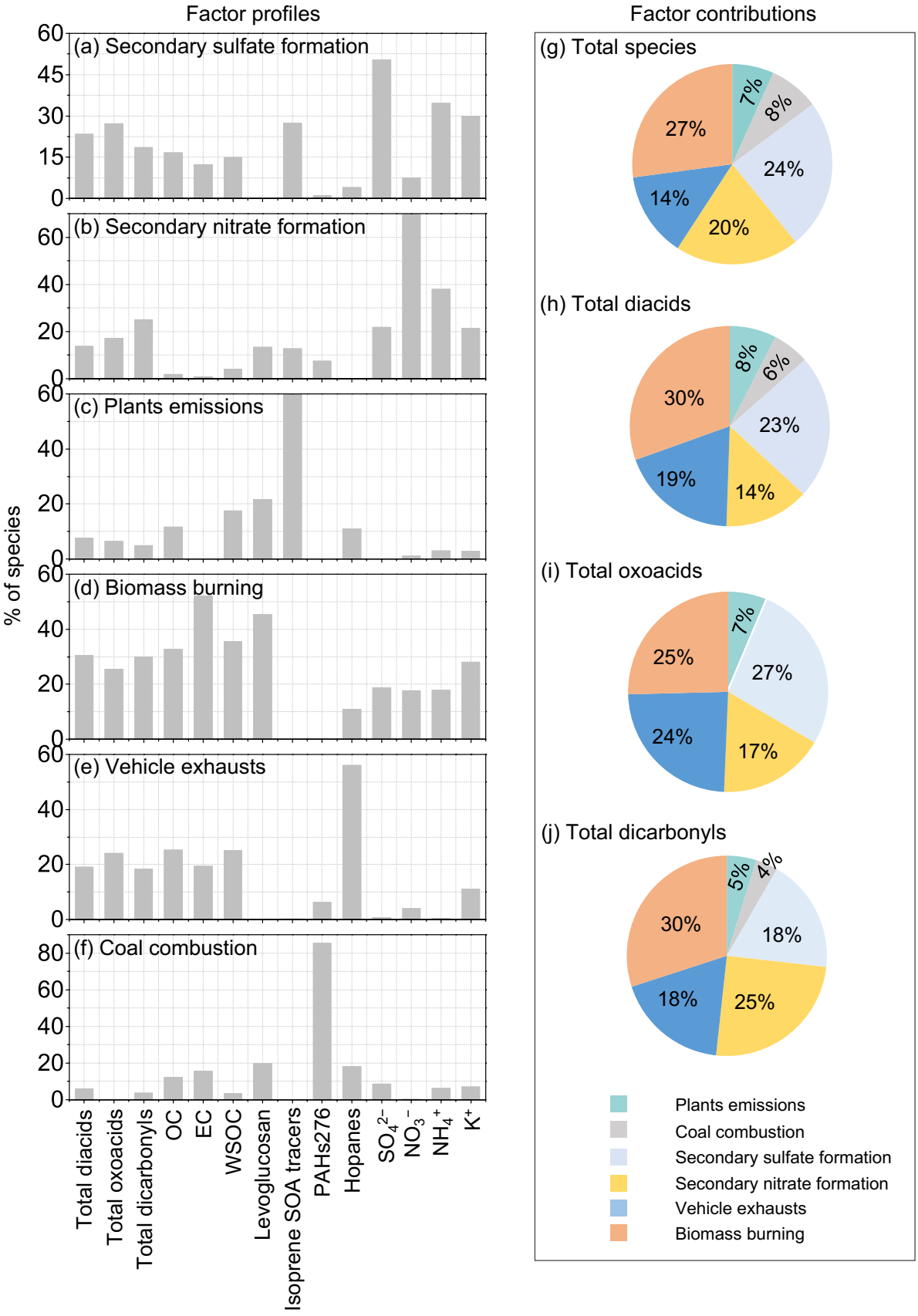

Figure 10. (a − f) Factor profiles (percentage of each species in factor) using ions and organics data for the six factors; (g − j) factor contributions to total species, diacids, oxoacids and α-dicarbonyls.